Copy 680

[redacted] NASA TM X-422

NASA TM X-422

[redacted]

Declassified by authority of NASA
Classification Change Notices No. 113
Dated

TECHNICAL MEMORANDUM

X-422

FULL-SCALE FLIGHT TEST FROM SEA LEVEL OF AN ABORT-ESCAPE SYSTEM FOR A PROJECT MERCURY CAPSULE

By Willard S. Blanchard, Jr., and James L. Raper

Langley Research Center
Langley Field, Va.

NATIONAL AERONAUTICS AND SPACE ADMINISTRATION

WASHINGTON October 1960

[redacted]

CONFIDENTIAL

NATIONAL AERONAUTICS AND SPACE ADMINISTRATION

TECHNICAL MEMORANDUM X-422

FULL-SCALE FLIGHT TEST FROM SEA LEVEL OF AN ABORT-ESCAPE SYSTEM FOR A PROJECT MERCURY CAPSULE*

By Willard S. Blanchard, Jr., and James L. Raper

SUMMARY

A system designed to provide safe escape for a Project Mercury manned space capsule during the atmospheric part of the boosted flight has been tested in free flight to determine its ability to function satisfactorily in the event of booster rocket malfunction at, or near, take-off. The configuration tested was a geometrically similar full-scale model of the Project Mercury capsule and escape system. The capsule was a body of revolution consisting of a large truncated cone with a spherical-segment base at the large diameter and a cylindrical canister surmounted by a small truncated cone at the small end. The escape system, consisting of a tower to which was mounted the escape rocket motor, was attached to the small end of the capsule. A small drogue parachute was used to deploy a large parachute which provided the low sinking rate required for safe landing.

The escape system performed satisfactorily. Maximum altitude attained was 1,950 feet. The main parachute provided at sea level a stabilized sinking rate of about 28 feet per second. The accelerations throughout the flight were within the tolerances of a properly positioned and supported human. The maximum sound level within the capsule (which was not insulated) was approximately 144 decibels during escape motor thrusting.

INTRODUCTION

The National Aeronautics and Space Administration is devoting considerable effort to the design of vehicles capable of safe manned orbital space flight and return. One such vehicle is the Project Mercury one-man space capsule. This vehicle consists of a conical-shaped capsule which will be mounted atop a large booster rocket motor. The capsule will reenter the earth's atmosphere large end forward in order to allow its large blunt heat shield to absorb the high heating rates associated with reentry from orbit. In addition to the high heating rates involved, high decelerations resulting from aerodynamic drag will be present during

*Title, Unclassified.

[redacted]

reentry. This, in turn, requires that the occupant be supported in a semisupine position with respect to the longitudinal axis of the capsule, in order to withstand the resultant high loads. It is required, therefore, in order to avoid excessive loads in an adverse (other than supine) direction on the occupant during the boosted, or accelerating, portion of the flight, that the capsule be mounted small end upstream during the boosted part of the flight.

It is imperative that a vehicle such as the Mercury capsule have a system capable of providing safe escape for the capsule in case of malfunction prior to the take-off or during thrusting of the booster rocket. During a relatively large portion of the boosted flight, where dynamic pressure is high, a stability problem exists if an abort-escape maneuver is required. Since the capsule (minus the abort-escape system) is designed to be aerodynamically stable large end forward during reentry (see ref. 1) but is boosted small end forward, the abort-escape system must, in addition to supplying the thrust required for rapid movement away from the booster, be capable of stabilizing the capsule small end forward in order to avoid the high transverse and adverse longitudinal loads that would be associated with an immediate turn-around at high dynamic pressure. Further, the abort-escape system must be capable of providing sufficient altitude for deployment of a landing parachute in event of booster rocket malfunction at, or near, take-off.

Small-scale tests conducted at the Langley Research Center showed that one promising method of stabilizing the capsule for the escape from the booster consisted of mounting the escape rocket motor on a tower from the small end of the capsule, thus moving the center of gravity sufficiently to provide aerodynamic stability when small end is forward. (See refs. 2 to 4.)

The Langley Research Center flight tested a full-scale model basically similar to the Project Mercury capsule to determine the ability of the abort-escape system to provide safe escape from sea level (simulating booster rocket malfunction at, or near, take-off). The results of this test (ref. 5) using an existing XM-19 Recruit rocket motor indicated that the basic system was workable. Subsequently, a capsule geometrically similar to the Project Mercury capsule and utilizing a Grand Central escape rocket motor developed expressly for the Mercury capsule was flown on a similar mission. Motions and resulting accelerations, along with sound level within the capsule during escape motor thrusting, were determined.

SYMBOLS

A_L	longitudinal accelerometer reading, g units
A_N	normal accelerometer reading, g units
A_T	transverse accelerometer reading, g units
A_Z	azimuth angle, deg
F	thrust, lb
g	acceleration due to gravity, 32.2 ft/sec^2
h	altitude, ft
I_Y	mass moment of inertia in pitch, slug-ft^2
I_Z	mass moment of inertia in yaw, slug-ft^2
M_Y	moment in pitch, ft-lb
M_Z	moment in yaw, ft-lb
N_{Re}	Reynolds number, based on maximum capsule diameter
p	free-stream static pressure, lb/sq ft
R	range, ft
R_x	range component along abscissa, ft
R_y	range component along ordinate, ft
T	free-stream temperature, $^{\circ}$F
t	time, sec
V	velocity along flight path, ft/sec
W	capsule weight, lb
x	station measured from maximum diameter, positive toward tower, in.

x_{cg} center-of-gravity station, measured from maximum diameter, in.

$\ddot{\theta}$ angular acceleration in pitch, radians/sec^2

$\ddot{\psi}$ angular acceleration in yaw, radians/sec^2

μ coefficient of viscosity, lb-sec/sq ft

ρ free-stream density, slugs/cu ft

MODEL

Figure 1 shows the general dimensions of the test model and related components. Figure 1(a) shows the dimensions of the test model as it was flown off the beach and the nomenclature used throughout this paper. Figure 1(b) gives detailed dimensions of the capsule which was used in the test. The maximum diameter of the capsule (80-inch spherical-radius base) was 74.5 inches. The spherical base was constructed of 3/16-inch steel plate reinforced with cross members of 5/16-inch steel plate. The conical sides of the capsule were constructed of 1/8-inch steel plate. The base and sides of the capsule simulated the shape of the final Project Mercury capsule but they were not intended to simulate the construction. A cylindrical canister 30 inches in diameter was placed on the small diameter of the conical capsule. A conical antenna fairing 20 inches in diameter at the smallest cross section was placed on the top of the main parachute compartment. The antenna fairing housed the drogue parachute and the antenna-fairing release mechanism.

Ballast was added to the capsule in order to locate the center of gravity at the proper station along the longitudinal axis; after which additional ballast was added symmetrically about the desired center of gravity, which was at station 19.5, in order to obtain the desired capsule weight of 2,169 pounds. The moments of inertia were approximately 485 slug-ft^2 in pitch and yaw and 236 slug-ft^2 in roll.

The tower, shown in figure 1(c), was constructed of steel tubes for main longitudinal members and horizontal and diagonal trusswork. The tower was attached to the capsule at the top of the canister by means of a segmented Marman clamp secured by three explosive bolts. A small tower jettison motor was employed to move the tower away from the capsule upon ignition of the three explosive bolts securing the Marman clamp to avoid entanglement of the tower with the parachute system. The jettison motor was mounted on the nozzle block between the three escape motor nozzles, as shown in figure 1(d). A conical blast shield was fitted over the antenna fairing and was intended to protect the top of the capsule from the tower jettison motor exhaust blast. The upper end of the tower was bolted to the nozzle block, shown in figure 1(d). Three 12° half-angle nozzles were attached to the nozzle block and were symmetrically spaced at intervals of 120°. The center line of each nozzle was canted 19° away from the center line of the test model in order to direct the rocket motor exhaust away from the capsule. The escape rocket motor was canted in order to obtain a misalinement of the thrust vector of 0.78 inch, to give the capsule a lateral displacement. Additional ballast was added to the upper end of the Grand Central motor to provide the desired launch center-of-gravity location (station 77.8). The mass characteristics of the capsule are shown in table I.

Two parachutes were employed. The first parachute deployed was a 72-inch-diameter nylon drogue parachute with a porosity of approximately 23 percent. The drogue parachute had a three-point connection to the antenna fairing and had a riser length of 30 feet. A 5-inch-diameter aluminum mortar was contained in the antenna fairing for ejecting the drogue parachute. The drogue parachute weighed approximately 7.5 pounds. The main parachute was a 64-foot ring sail type with porosity of about 15 percent, had a single-point suspension, a shroud length of 60 feet, a riser length of 6 feet, and was not reefed. The main parachute was packaged in a deployment bag which made a free-sliding fit in an aluminum can 40 inches long located in the canister and extending 21 inches down into the capsule. The main parachute weighed approximately 60 pounds. Reference 6 presents additional flight tests of the main parachute. The canister also contained a main-parachute release mechanism which was actuated when the capsule impacted with the water. Figure 1(e) shows the orientation of the drogue and main parachutes.

INSTRUMENTATION

Two "g" actuated timers connected in parallel were used to program the ignition of the Marman clamp explosive bolts, ignition of the tower jettison motor, ignition of the drogue mortar, and ignition of the explosive bolt retaining the antenna fairing.

Four GSAP 16-millimeter cameras were carried onboard the capsule for the purpose of observing the tower and rocket motor burning and for obtaining a "pilot's view" from the capsule. Figure 1(f) shows the location of the cameras, three of which pointed up and one of which pointed down.

Two onboard recorders recorded the sound level during the flight.

Flight-path data were obtained by continuous tracking of the model with an FPS-16 tracking radar, an NASA modified SCR 584 tracking radar, and a commercially modified SCR 584 radar. Velocity along the trajectory was determined by CW Doppler velocimeter up to deployment of the main parachute. The velocity of descent with the main parachute opened was obtained from the time-history variations of the trajectory as determined by the FPS-16 radar. Motion pictures of the flight were taken by cameras located near the launching site.

A six-channel telemeter was employed to transmit normal, transverse, and longitudinal accelerations at two longitudinal positions to ground receiving stations. As shown in figure 2(a), the accelerometers were located on the capsule center line at approximately 20 and 52 inches from the capsule maximum diameter.

TEST

Prior to assembly of the model on the launch pad, a temperature-sensitive paint was applied to the exterior of the model at several locations in order to determine whether and where regions of high heat flux resulting from the rocket exhaust existed. The paint was applied to the legs and cross members of the tower at various longitudinal positions, to the conical sides of the antenna fairing, to the sides of the canister, and at various longitudinal positions along the capsule. The transition temperatures of the paints used ranged between approximately 150° F and $1,300^{\circ}$ F.

Figure 3 shows the model on the launcher prior to take-off. The model was launched at an elevation angle of 71° to insure a water impact. The variation of free-stream density, pressure, temperature, and coefficient of viscosity for the flight test are shown in figures 4 and 5. The flight-test Reynolds number, shown in figure 6, based on maximum capsule diameter, varied from approximately 22×10^{6} at escape motor tail off to 1.1×10^{6} during main parachute descent. The time-history variation of weight and center of gravity of the test model is shown in figure 7.

Ground static tests of the tower jettison motor and the escape motor were performed prior to the current test in order to obtain typical thrust-time curves of the respective motors. Results of these tests are shown in figures 8 and 9, respectively.

RESULTS AND DISCUSSION

Sequence photographs, showing the principal events in the flight test, are presented in figure 10. Take-off and powered flight, shown in sequence photographs 1, 2, and 3, occurred with the model experiencing very little flight-path deviation. At the time corresponding to separation of the escape tower (photograph 4) the model had experienced approximately $1\frac{1}{4}$ revolutions in pitch and about 1/8 revolution in yaw. This motion was due primarily to the deliberate escape motor thrust misalinement and the lack of damping of the model in the abort configuration. The purpose of this misalinement was to displace the capsule from the path of the booster in later boosted flights. In the latter part of the pitching revolution during motor tail off (thrust decay), the model started to yaw. After tower separation, the capsule continued to tumble until the drogue parachute was deployed and partially stabilized the capsule as shown in sequence photographs 5, 6, and 7. Sequence photographs 8 and 9 show the main parachute after it was pulled out by the drogue parachute and the antenna fairing. The main parachute stabilized the capsule and lowered it to the water. At impact with the water the main parachute was automatically released. The capsule floated with its longitudinal axis nearly horizontal after impact. Unpublished data indicate that the capsule was capable of maintaining a vertical attitude only if it did not exceed a 30° tilt on landing. This condition was exceeded as a result of the wind drift at landing. The capsule was recovered by a Marine helicopter shortly after it impacted with the water, as seen in figure 11. The tower and antenna fairing were recovered by a U.S. Navy underwater demolition team.

The motion pictures obtained from the three up-cameras showed that motor burning was normal and that the tower separated without any apparent interference. Examination of the temperature-sensitive paint on the capsule and tower showed no evidence of heating sufficient to be indicated by the lowest range paint (150° F). Examination of the onboard recorder records showed that the maximum sound level was approximately 144 decibels during escape motor burning; this condition indicated a need for insulation against noise for manned flights.

An isometric view of the flight trajectory showing the principal events during the flight is shown in figure 12. The variations of altitude with range, altitude with time, and a horizontal projection of the trajectory are shown in figures 13, 14, and 15, respectively. The escape motor burned out at an altitude of approximately 300 feet and the tower was separated at an altitude of about 1,850 feet. The drogue parachute was deployed at an altitude of about 1,900 feet and a velocity of about 95 feet per second. The main parachute was fully opened at an altitude of about 1,500 feet and a velocity of about 90 feet per second; thus, ample time was allowed for the sinking speed to stabilize. Impact occurred at approximately 1,600 feet from take-off after about 63.1 seconds of flight time. Figure 16 shows the variation of velocity along the flight path and the vertical component of velocity with time. The maximum velocity occurred at escape motor tail off and was about 595 feet per second. Rate of descent was about 28 feet per second at sea level (impact), which agreed with expected performance of the parachute.

The time-history variation of longitudinal, normal, and transverse accelerations as measured by the accelerometers is presented in figure 17. The accelerations at station 20 are approximately those which would be experienced by an occupant during an escape maneuver. The maximum longitudinal acceleration was approximately 22g and lasted for about 0.1 second. The maximum accelerations after burnout (about 1.2 seconds) and prior to impact did not exceed ±5g in any direction. Time-history plots of acceleration after 24 seconds were omitted from figure 17 because the variations of accelerations were small (less than ±1g). Based on references 7 to 11, the loads encountered throughout this flight were within the tolerance of a properly positioned and supported occupant. Accelerometer values at impact have been omitted because the frequency response of the accelerometers was not adequate to determine the loads at impact.

The normal and transverse accelerometer readings at the two longitudinal stations were indicative of the angular accelerations in pitch and yaw. The angular accelerations presented in figure 18 were determined from the following expressions:

$$\ddot{\theta} = 32.2\left(\frac{A_{N_{52}} - A_{N_{20}}}{x_{52} - x_{20}}\right) \times 12$$

and

$$\ddot{\psi} = 32.2\left(\frac{A_{T_{52}} - A_{T_{20}}}{x_{52} - x_{20}}\right) \times 12$$

where subscripts 52 and 20 refer to longitudinal stations.

The maximum angular accelerations were about 6 radians/sec^2 during the thrusting period of the escape motor and about 40 radians/sec^2 during main parachute opening. After the main parachute opened and the descending capsule stabilized, the maximum angular acceleration was about 20 radians/sec^2.

It should be noted that large percentage errors in $\ddot{\theta}$ and $\ddot{\psi}$ are likely when the differences in the accelerations at the two stations are small. However, the angular accelerations are also small in these cases.

The pitching and yawing moments during the flight were proportional to the $\ddot{\theta}$ and $\ddot{\psi}$ values given in figure 18 and may be determined from:

$$M_Y = I_Y\ddot{\theta}$$

and

$$M_Z = I_Z\ddot{\psi}$$

The maximum moment was obtained at 1.1 seconds after launch and was approximately 37,000 foot-pounds in pitch. The largest moment obtained after the main parachute opened was approximately 18,000 foot-pounds in pitch.

CONCLUSIONS

The system proposed to provide safe abort escape for a Project Mercury manned space capsule has been investigated by a full-scale flight test to determine its ability to provide safe escape for the capsule in the event of booster rocket malfunction at, or near, take-off. The test results indicate the following conclusions:

1. The maximum accelerations about the three axes were within the tolerance of a properly positioned and supported human.

2. The escape motor provided sufficient altitude for successful opening of the landing parachute.

3. The stabilized rate of descent of the capsule (parachute fully open) was about 28 feet per second at sea level.

4. The maximum sound level within the capsule was about 144 decibels during escape motor burning and indicated the need for insulation against sound.

5. There were no indications of high temperatures on the escape tower or the capsule as a result of escape motor exhaust.

Langley Research Center,
National Aeronautics and Space Administration,
Langley Field, Va., June 29, 1960.

[redacted]

REFERENCES

1. Scallion, William I.: Full-Scale Wind-Tunnel Investigation of the Low-Speed Static Aerodynamic Characteristics of a Model of a Reentry Capsule. NASA TM X-220, 1959.

2. Johnson, Joseph L, Jr.: Wind-Tunnel Investigation at Low Subsonic Speeds of the Static and Oscillatory Stability Characteristics of Models of Several Space Capsule Configurations. NASA TM X-285, 1960.

3. Pearson, Albin O.: Wind-Tunnel Investigation at Mach Numbers From 0.50 to 1.14 of the Static Aerodynamic Characteristics of a Model of a Project Mercury Capsule. NASA TM X-292, 1960.

4. Shaw, David S., and Turner, Kenneth L.: Wind-Tunnel Investigation of Static Aerodynamic Characteristics of a 1/9-Scale Model of a Project Mercury Capsule at Mach Numbers From 1.60 to 4.65. NASA TM X-291, 1960.

5. Blanchard, Willard S., Jr., and Hoffman, Sherwood: Full-Scale Flight Test of a Proposed Abort-Escape System for a Manned Space Capsule From Sea Level. NASA TM X-351, 1960.

6. Kurbjun, Max C.: High-Altitude Performance of a 64-Foot-Diameter Ring Sail Parachute. NASA TM X-232, 1959.

7. Clark, Carl C., and Gray, R. Flanagan: A Discussion of Restraint and Protection of the Human Experiencing the Smooth and Oscillating Accelerations of Proposed Space Vehicles. MA-5914, Aviation Medical Acceleration Lab., U.S. Naval Air Dev. Center (Johnsville, Pa.), Dec. 1959.

8. Collins, C. C., Crosbie, R. J., and Gray, R. F.: Pilot Performance and Tolerance Studies of Orbital Re-entry Acceleration. MA-8, Aviation Medical Acceleration Lab., U.S. Naval Air Dev. Center (Johnsville, Pa.), Sept. 1958.

9. Collins, C. C., and Gray, R. F.: Pilot Performance and Tolerance Studies of Orbital Re-entry Acceleration. MA-1.1, Aviation Medical Acceleration Lab., U.S. Naval Air Dev. Center (Johnsville, Pa.), Sept. 1959.

10. Lombard, Charles F.: Human Tolerance to Forces Produced by Acceleration. Rep. No. ES21072, Douglas Aircraft Co., Inc., Feb. 27, 1948.

11. Smedal, Harold A., Stinnett, Glen W., and Innis, Robert C.: A Restraint System Enabling Pilot Control Under Moderately High Acceleration in a Varied Acceleration Field. NASA TN D-91, 1960.

TABLE I

CAPSULE MASS CHARACTERISTICS

Condition	Weight, lb	x_{cg}, in.
Take-off	3,109	77.8
Burnout	2,819	63.2
Capsule alone	2,169	19.5
Capsule after landing	2,048	16.7
Take-off inertias:		
Pitch or yaw, slug-ft^2		6,100
Roll, slug-ft^2		330
Burnout inertias:		
Pitch or yaw, slug-ft^2		4,770
Roll, slug-ft^2		330
Capsule alone inertias:		
Pitch or yaw, slug-ft^2		485
Roll, slug-ft^2		236

L-1133

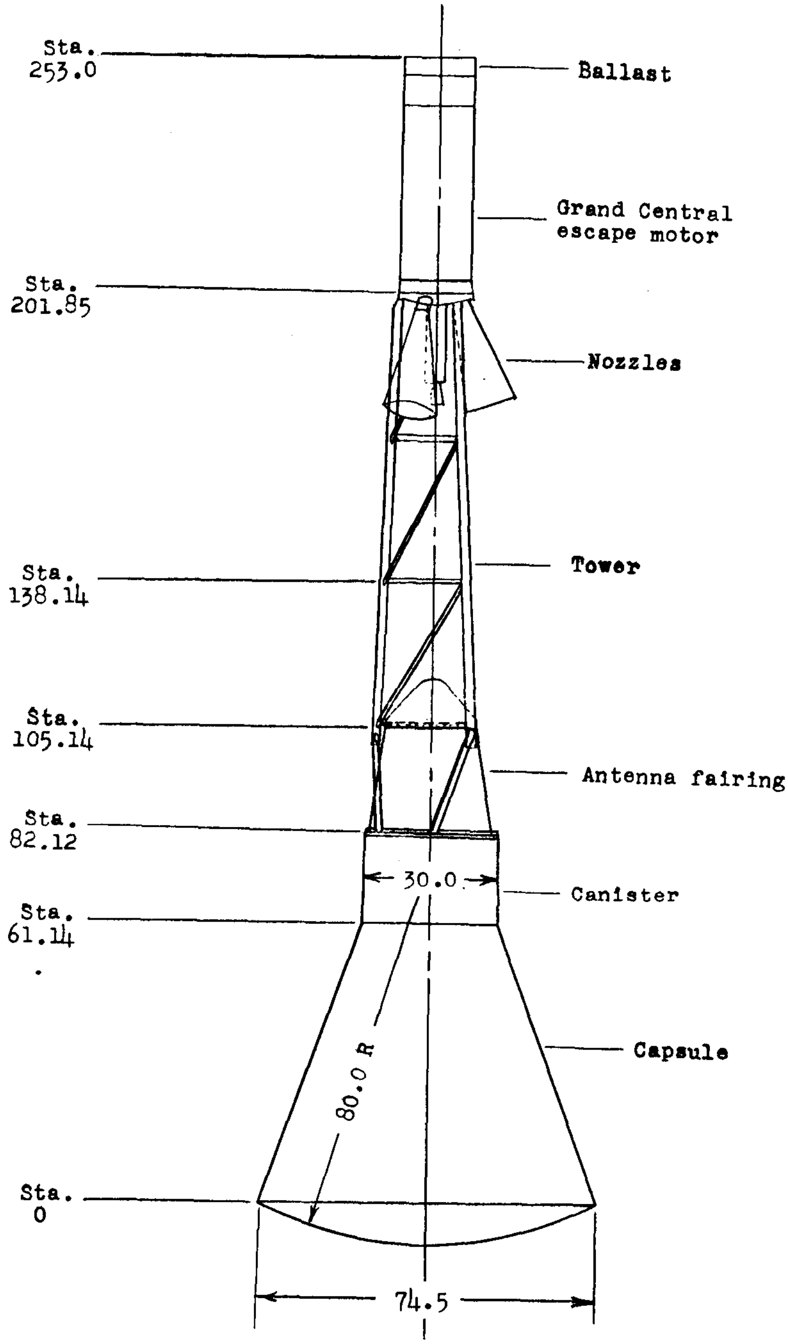

(a) Principal dimensions and nomenclature of the vehicle tested.

Figure 1.- Drawings of model and components. All dimensions are in inches.

[redacted]

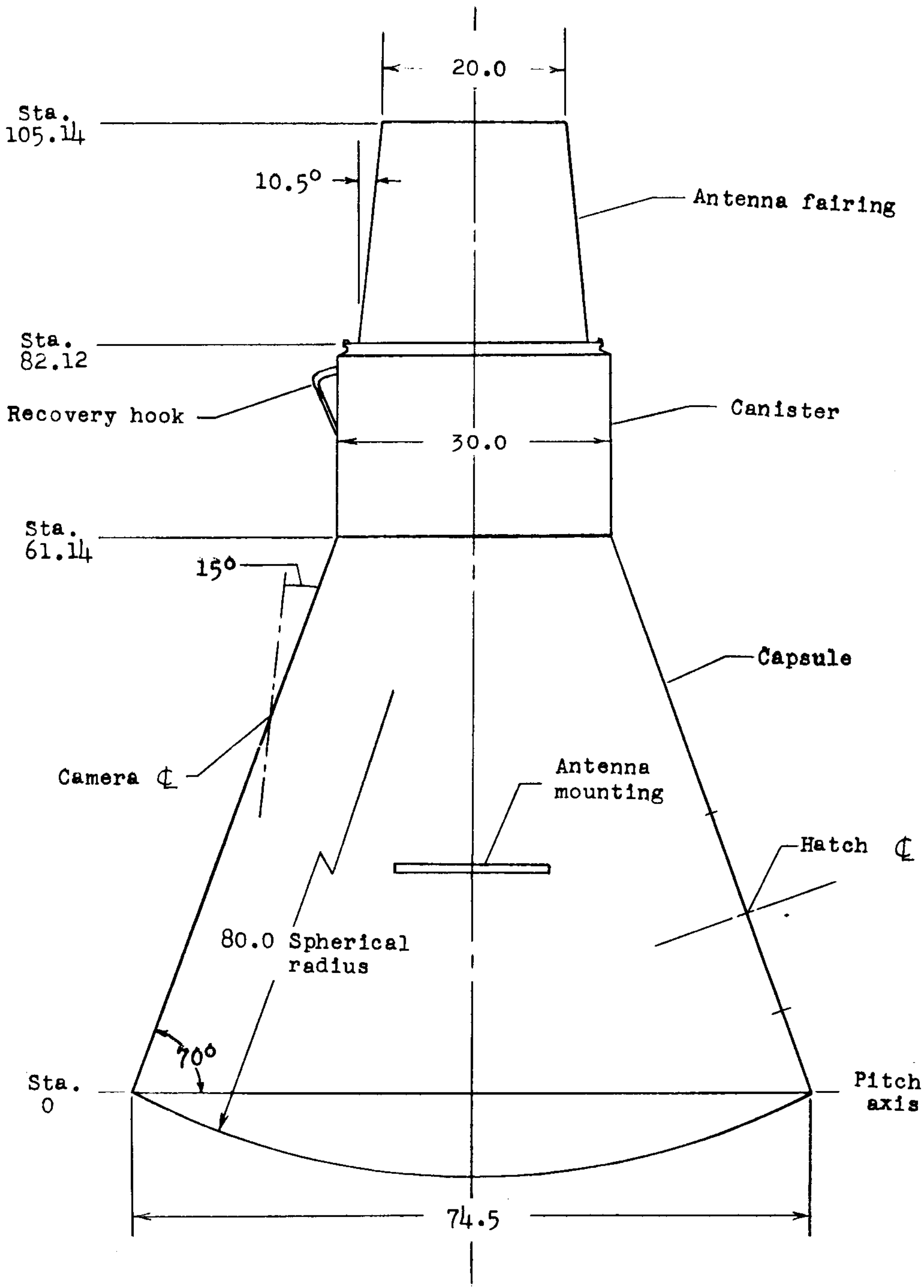

(b) Dimensions of the capsule.

Figure 1.- Continued.

[redacted]

L-1133

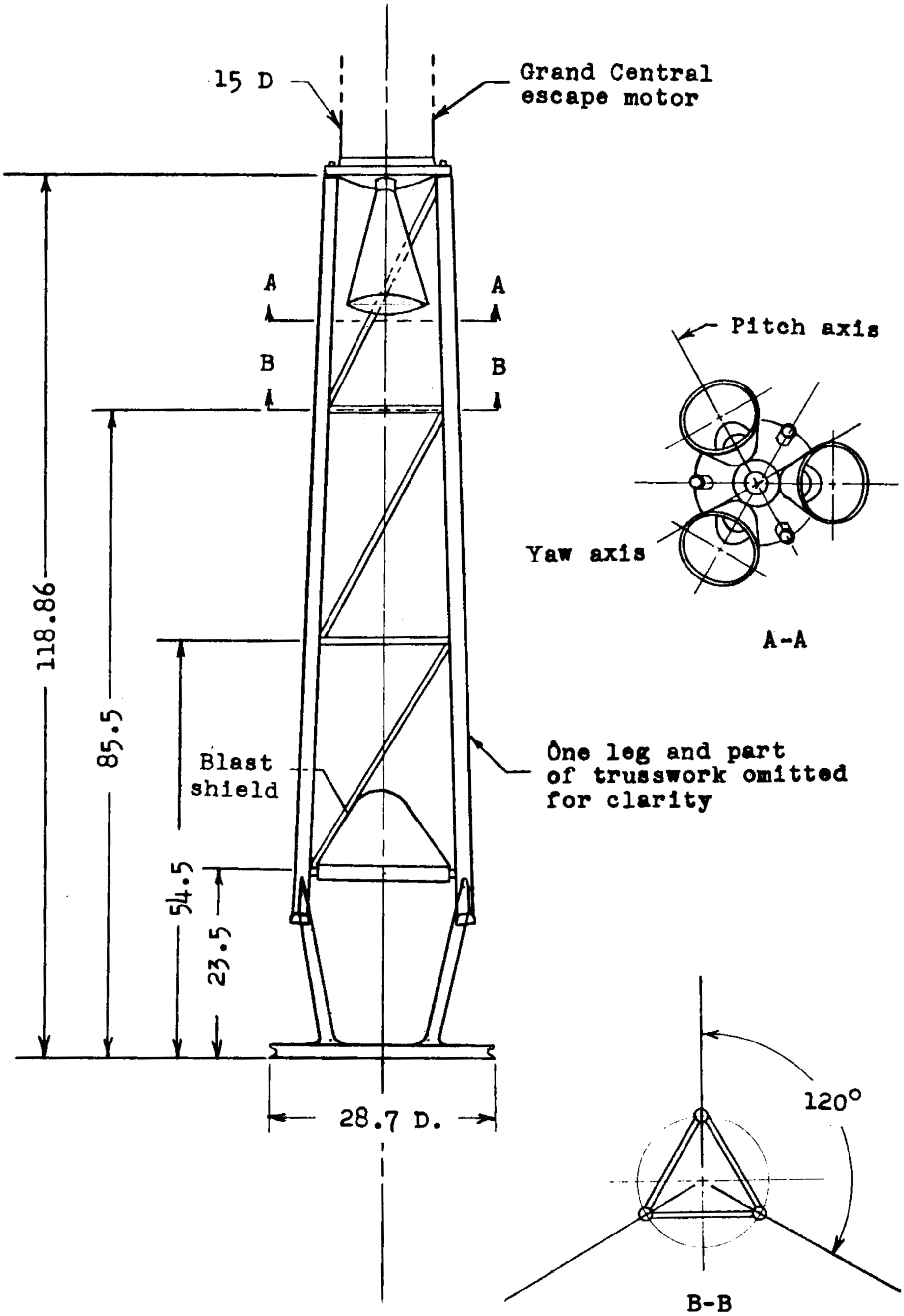

(c) Dimensions and details of tower.

Figure 1.- Continued.

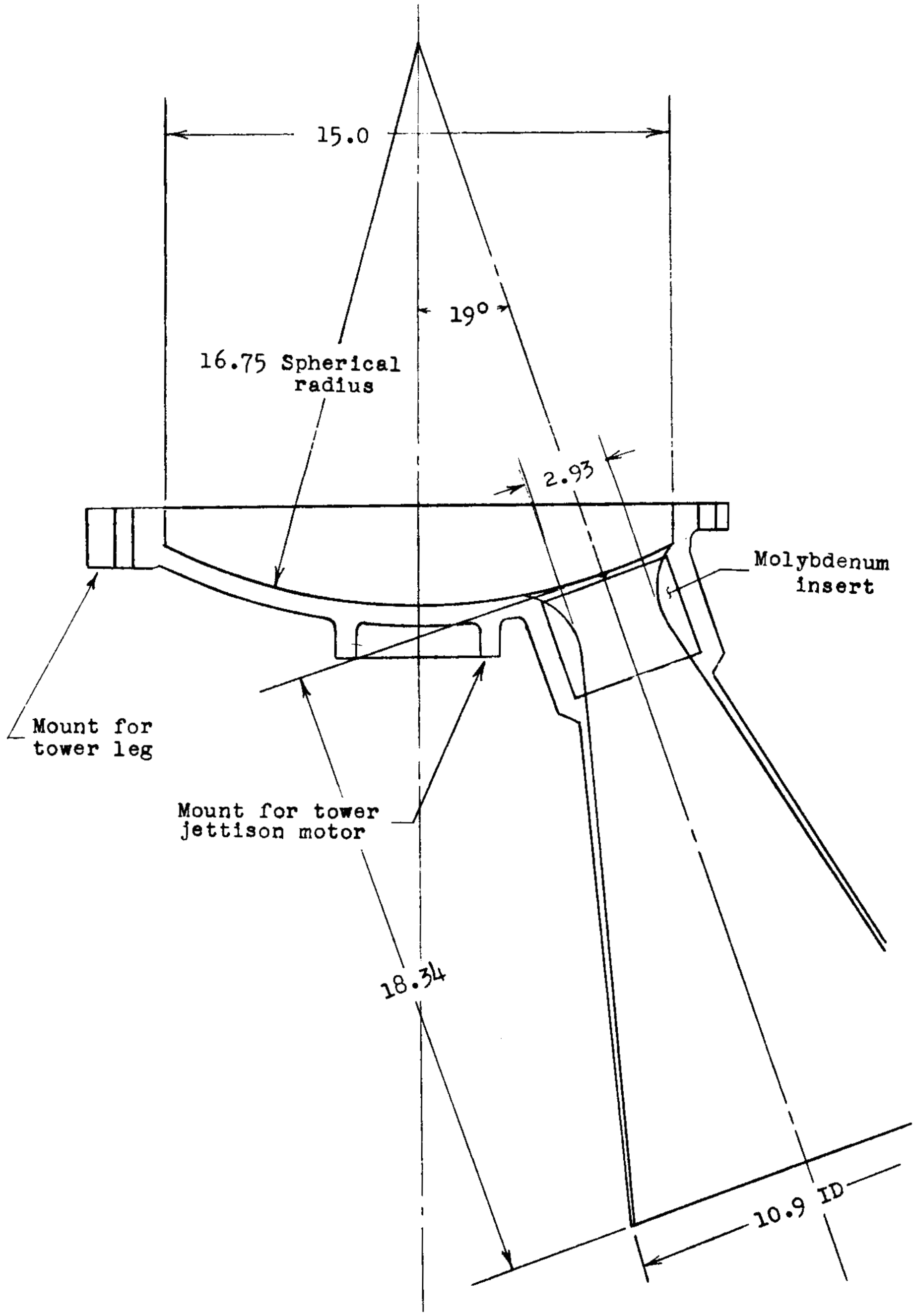

(d) Nozzle and nozzle mounting block details.

Figure 1.- Continued.

[redacted]

Y

L-1133

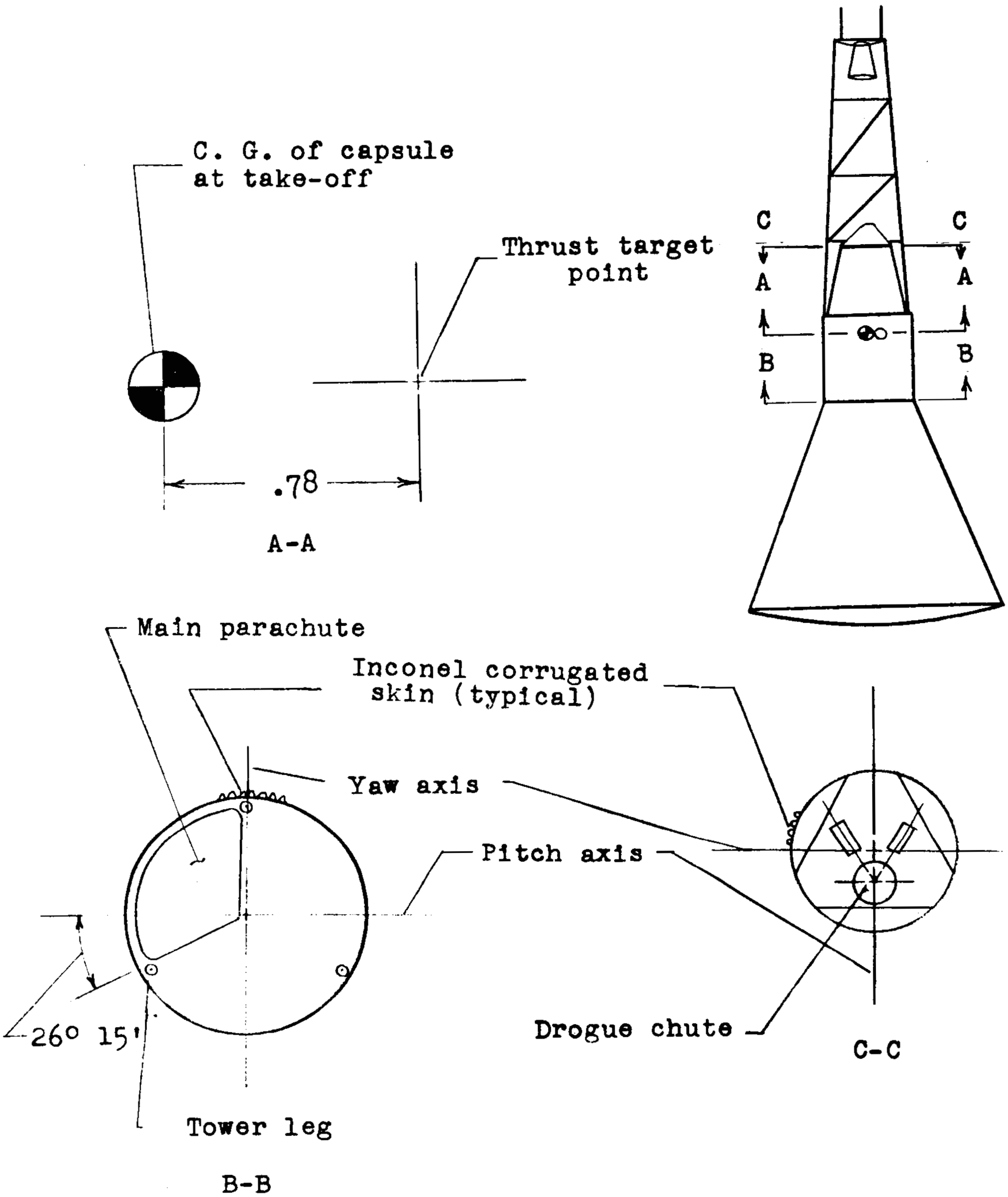

(e) Cross-sectional views showing thrust misalinement, main parachute arrangement, drogue parachute arrangement, and axis notation.

Figure 1.- Continued.

[redacted]

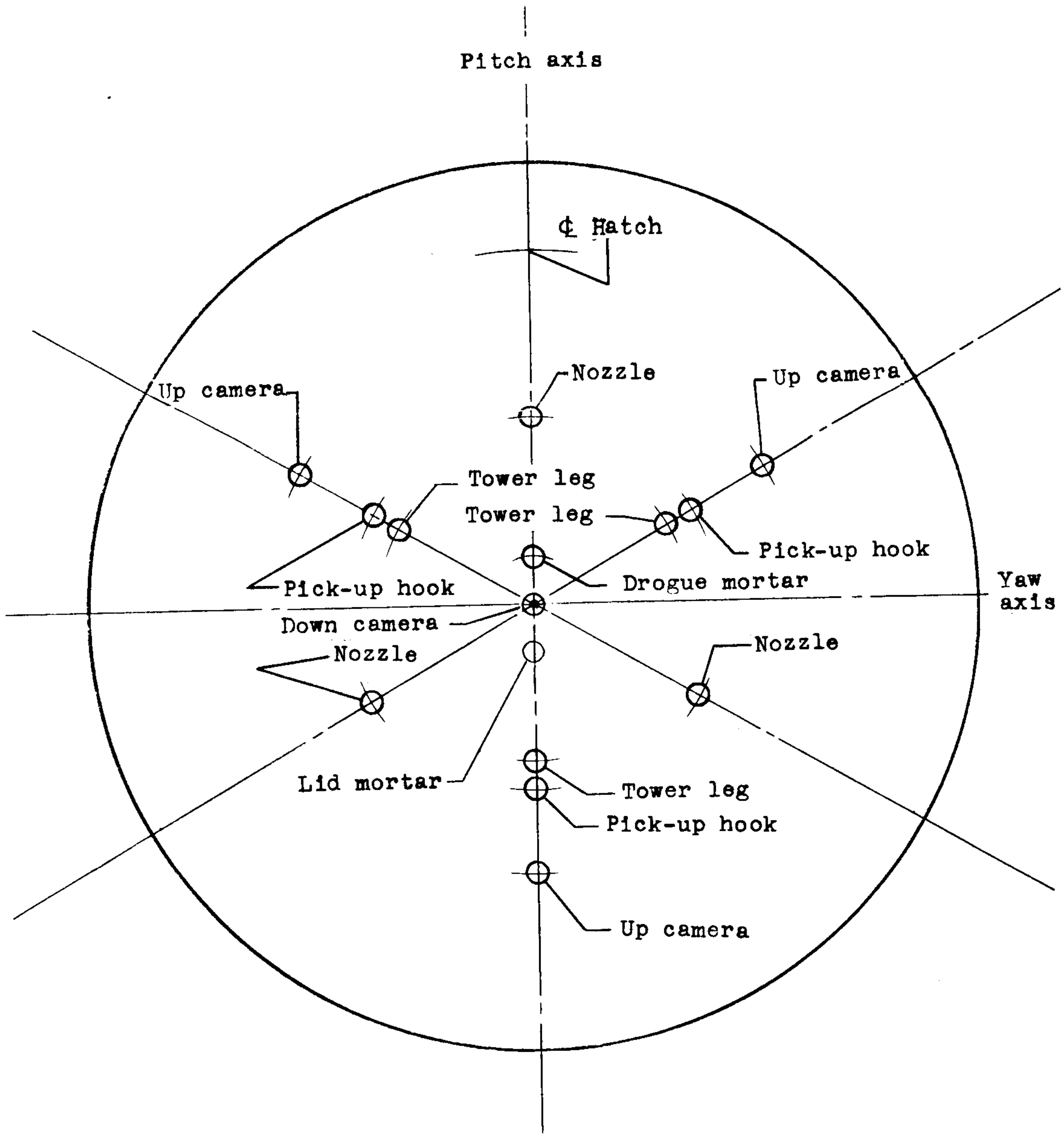

(f) Orientation schematic diagram of test capsule.

Figure 1.- Concluded.

L-1133

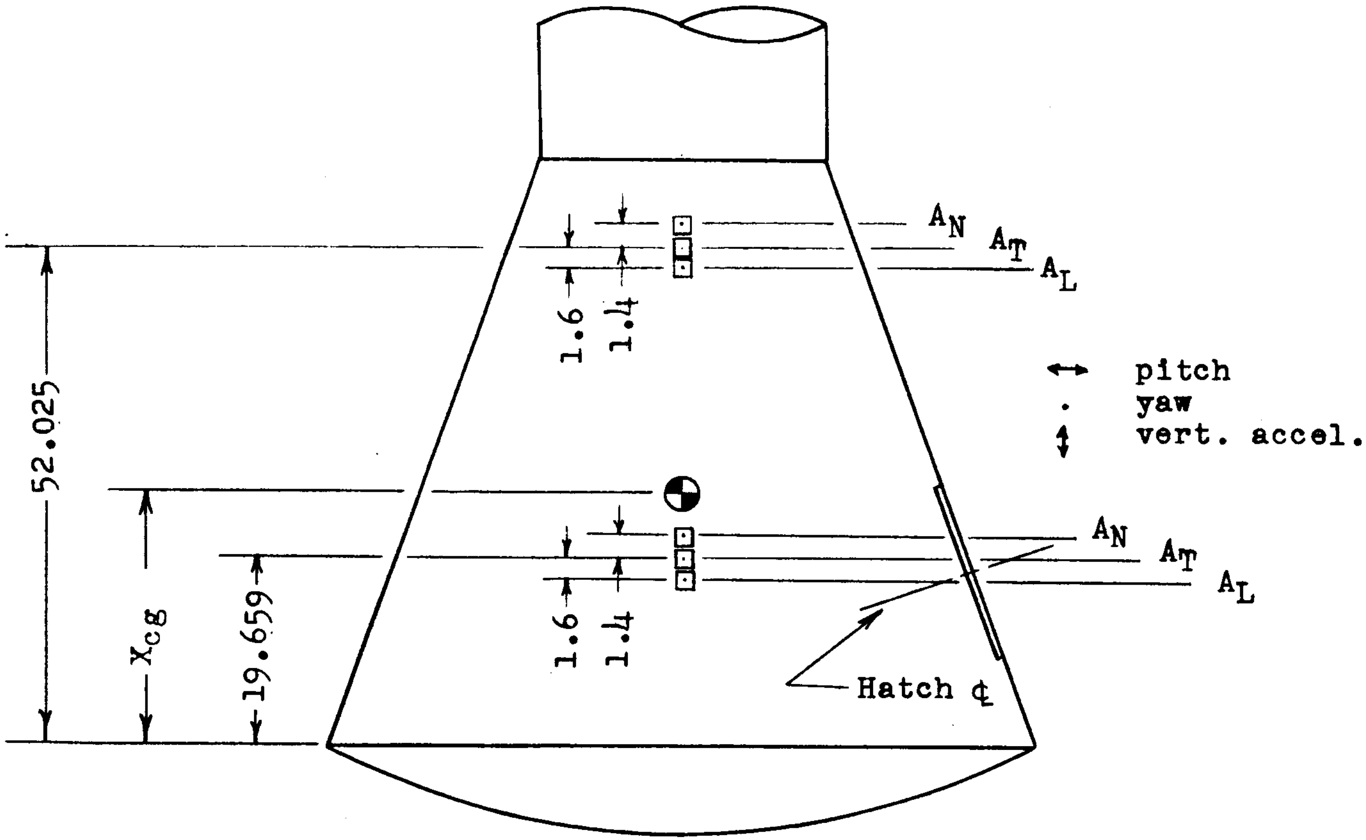

Figure 2.- Capsule accelerometer locations. All accelerometers are on center line.

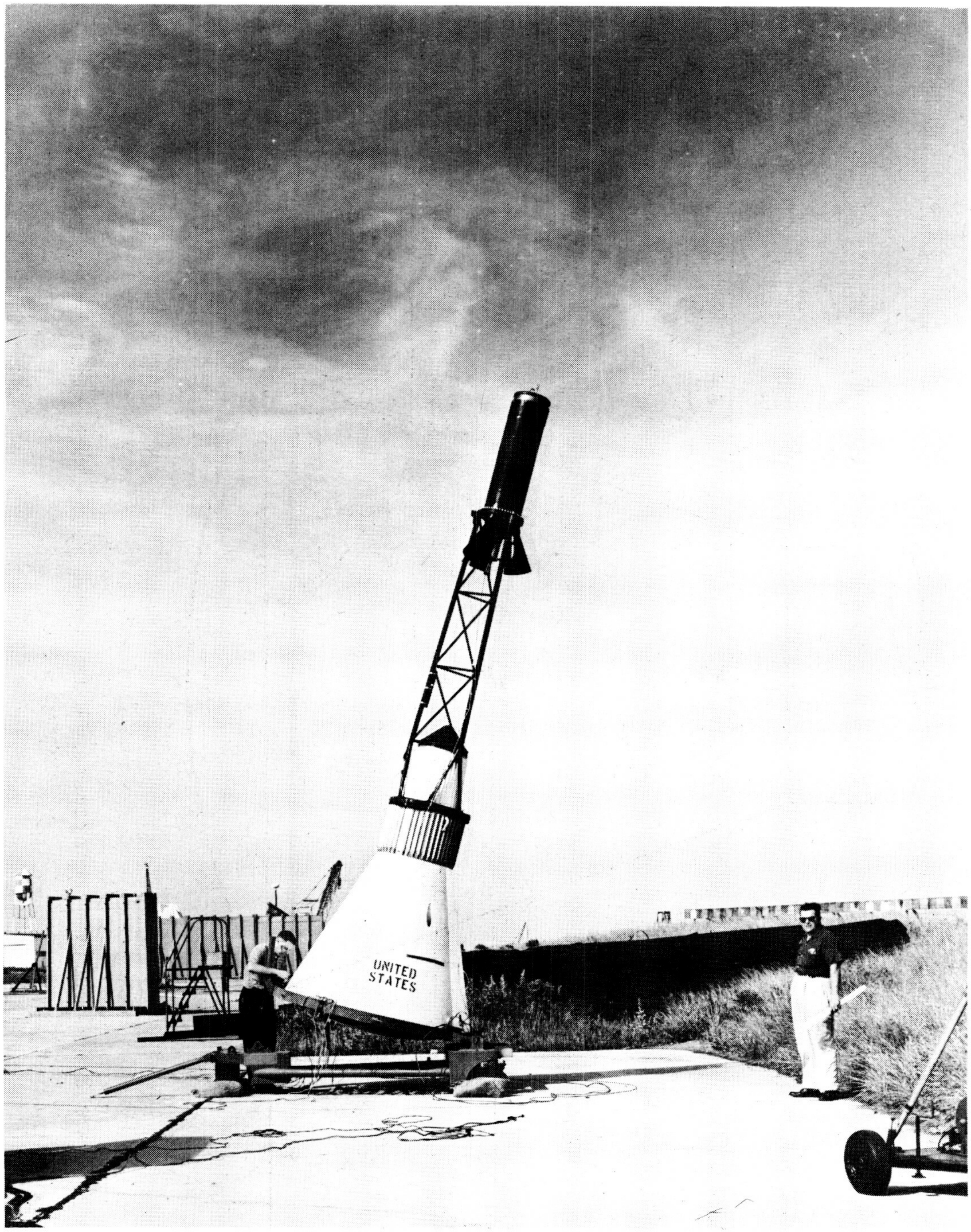

Figure 3.- Photograph of capsule and launcher. L-59-5120

L-1133

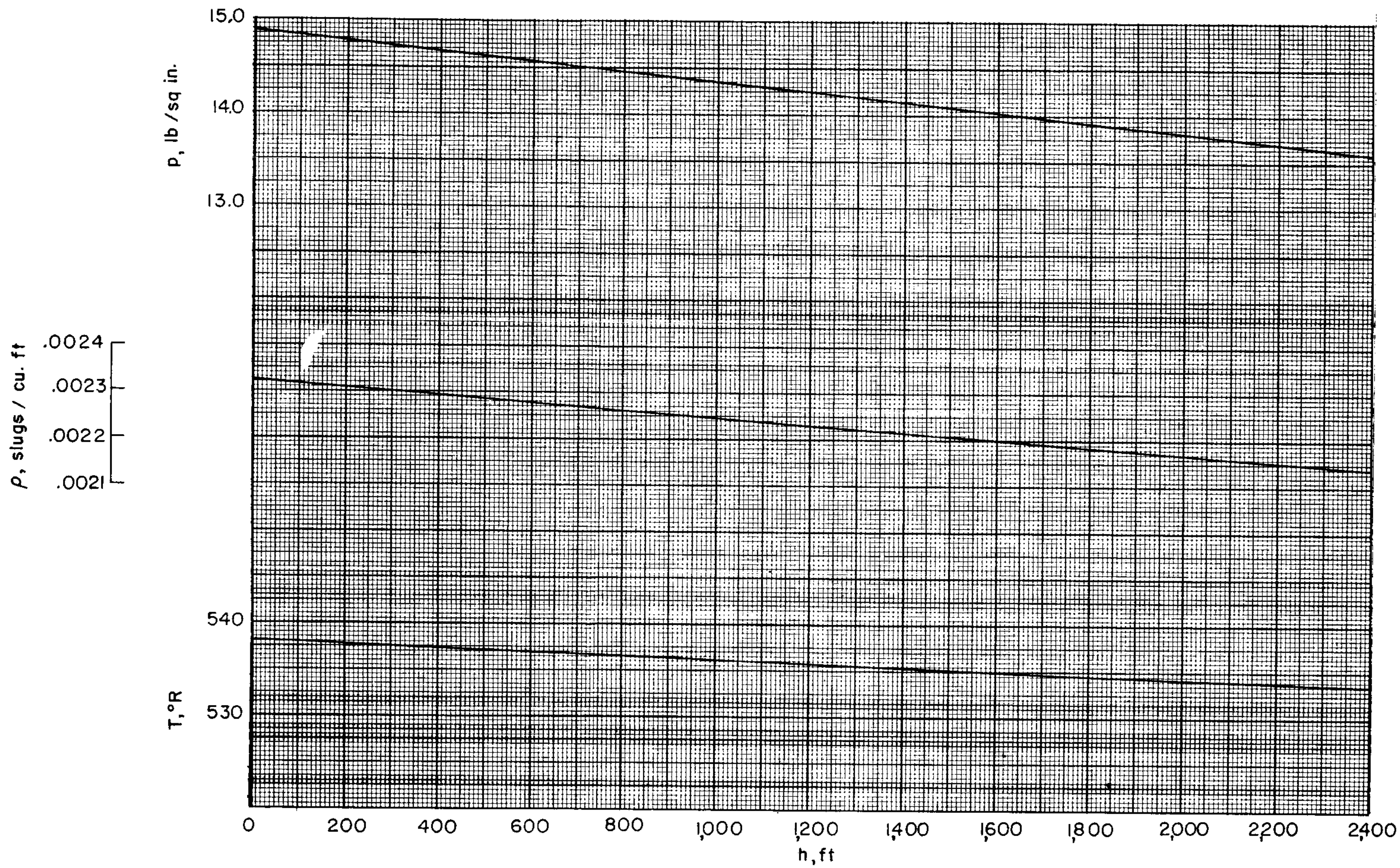

Figure 4.- Variation of temperature, density, and pressure with altitude.

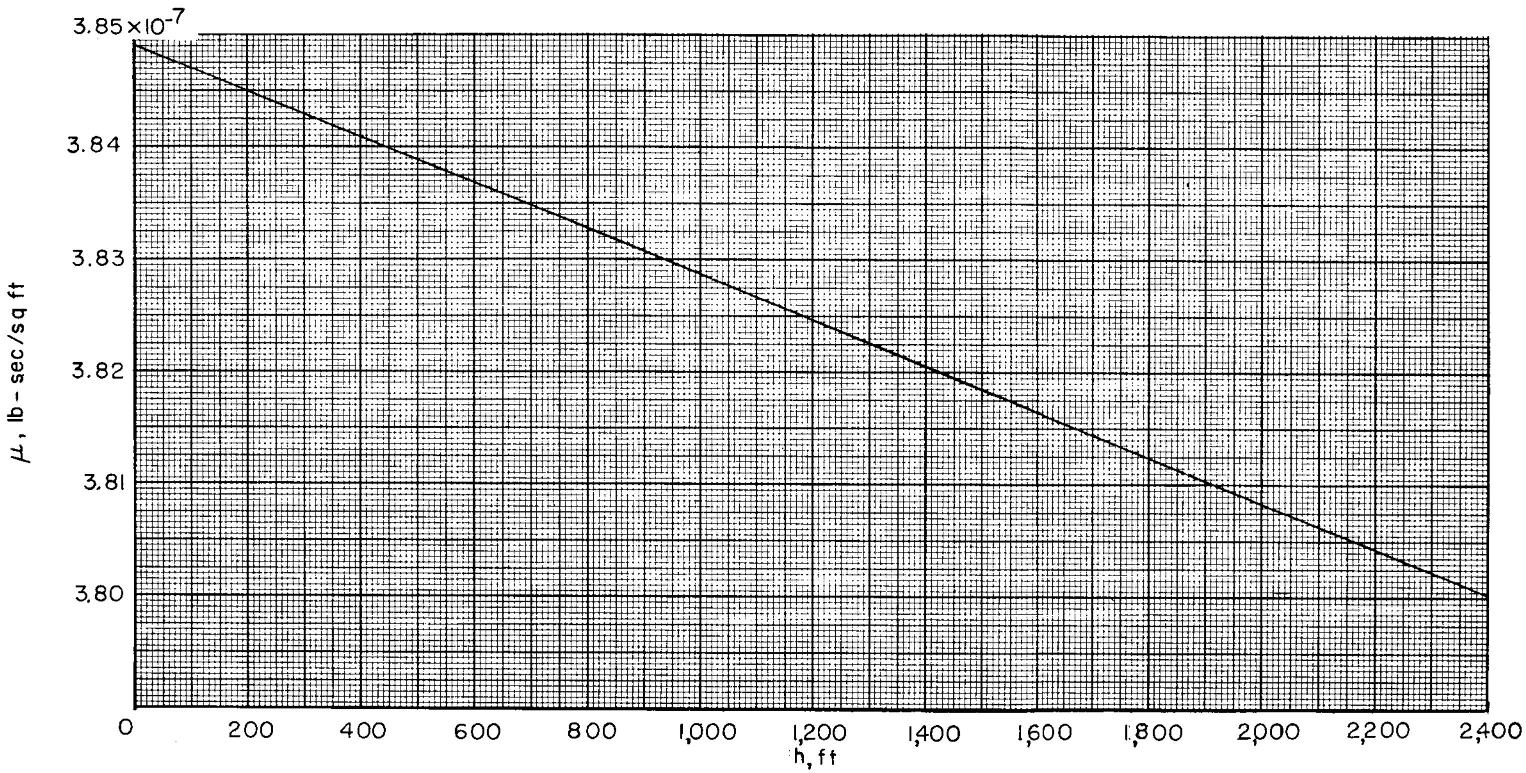

Figure 5.- Variation of coefficient of viscosity with capsule altitude.

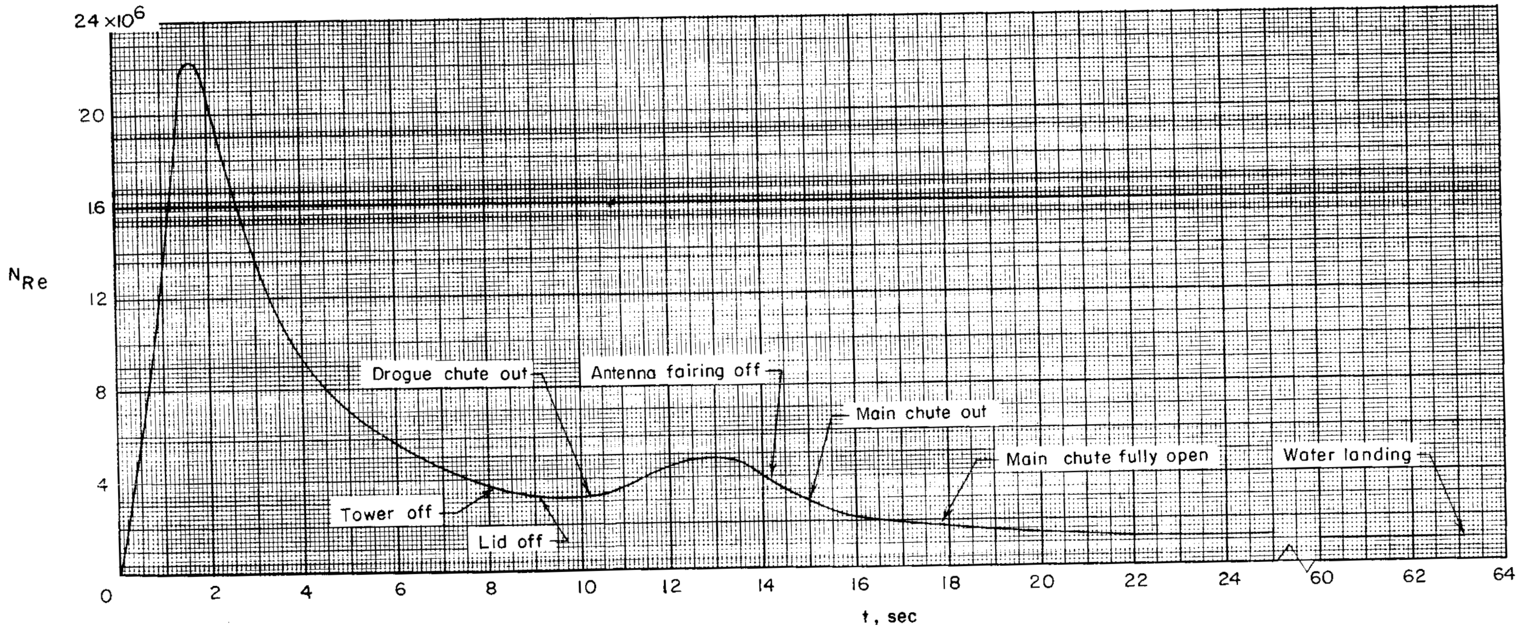

Figure 6.- Variation of Reynolds number with time.

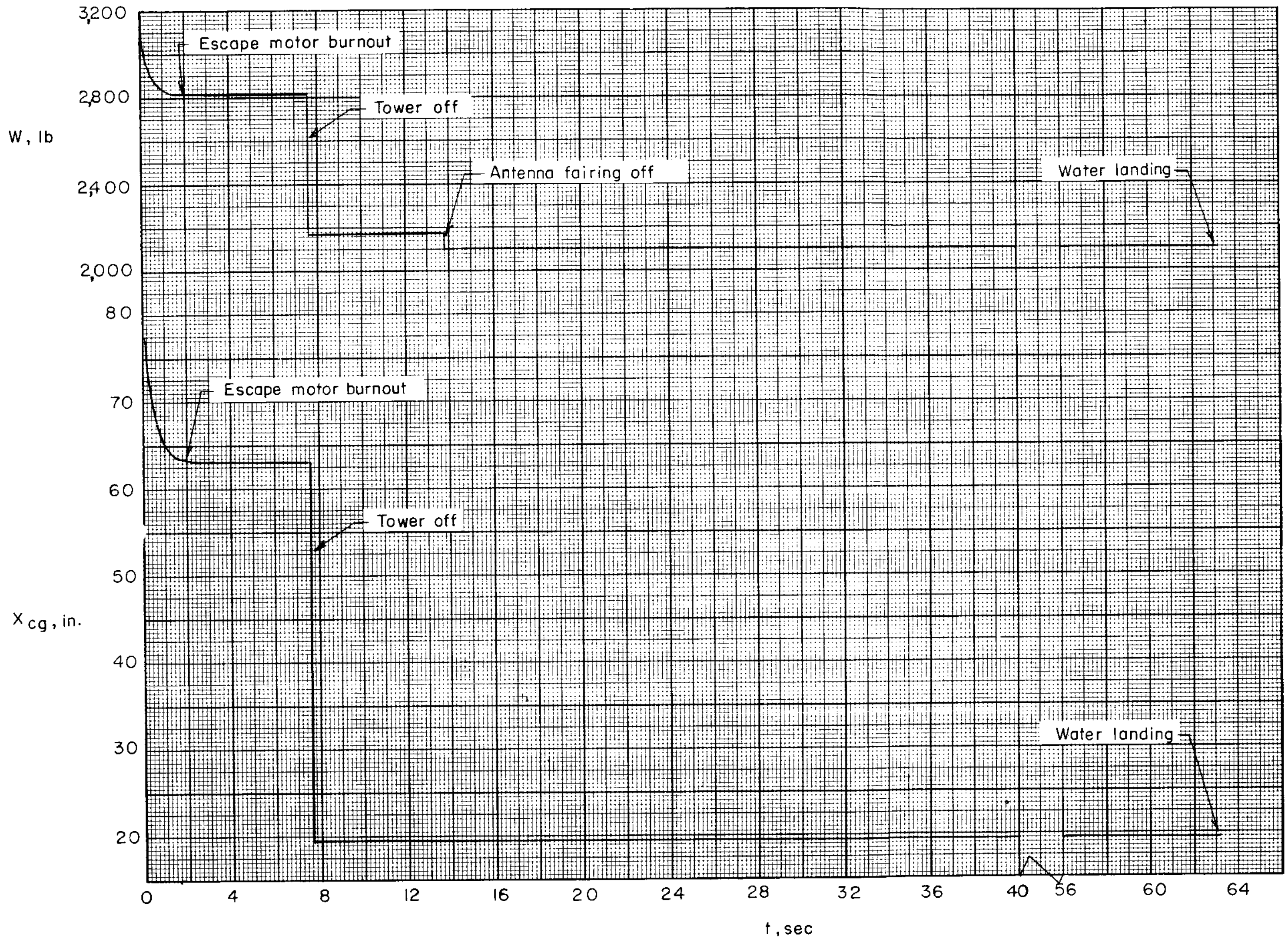

Figure 7.- Variation of capsule weight and center of gravity with time.

L-1133

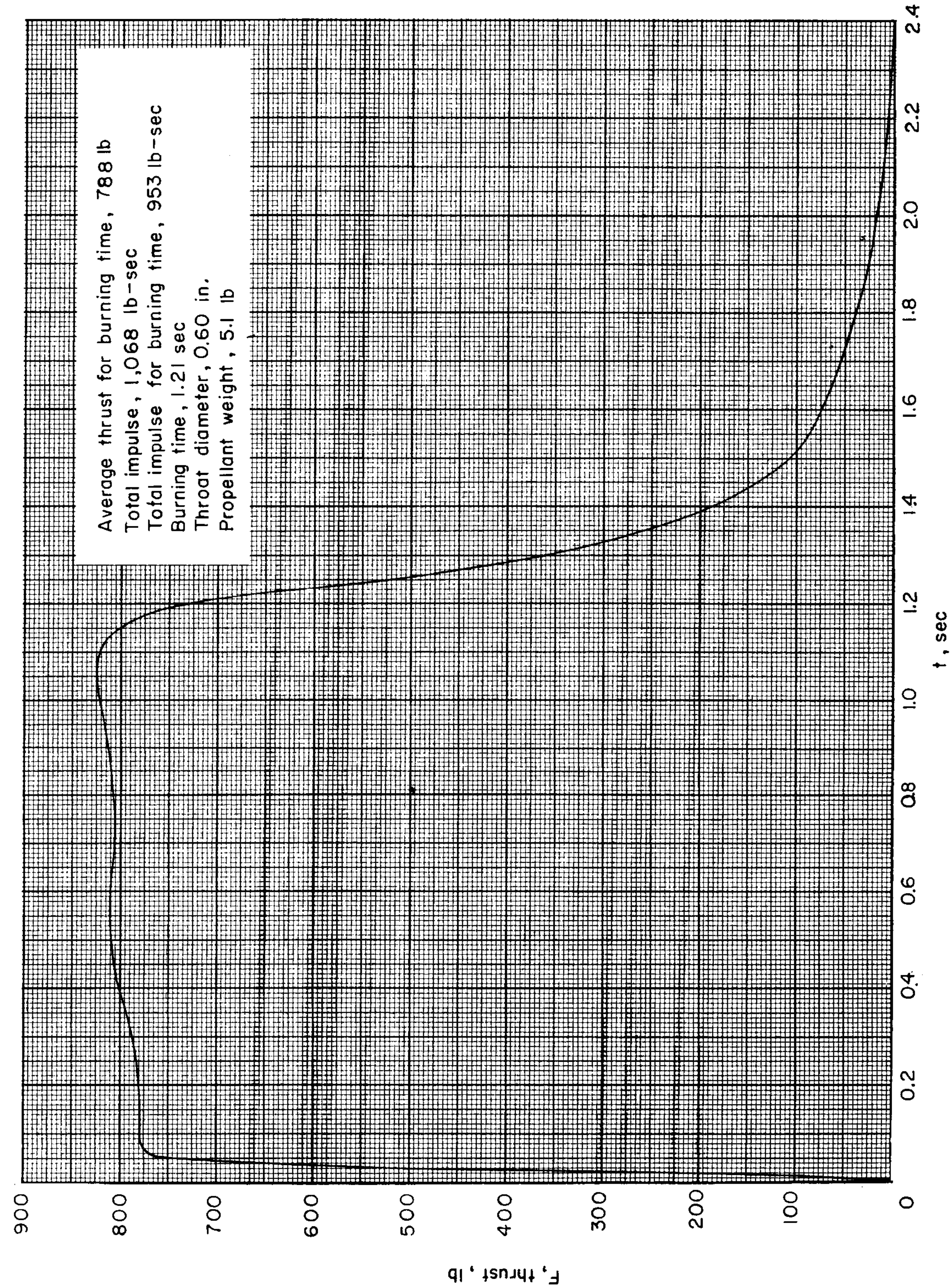

[redacted]

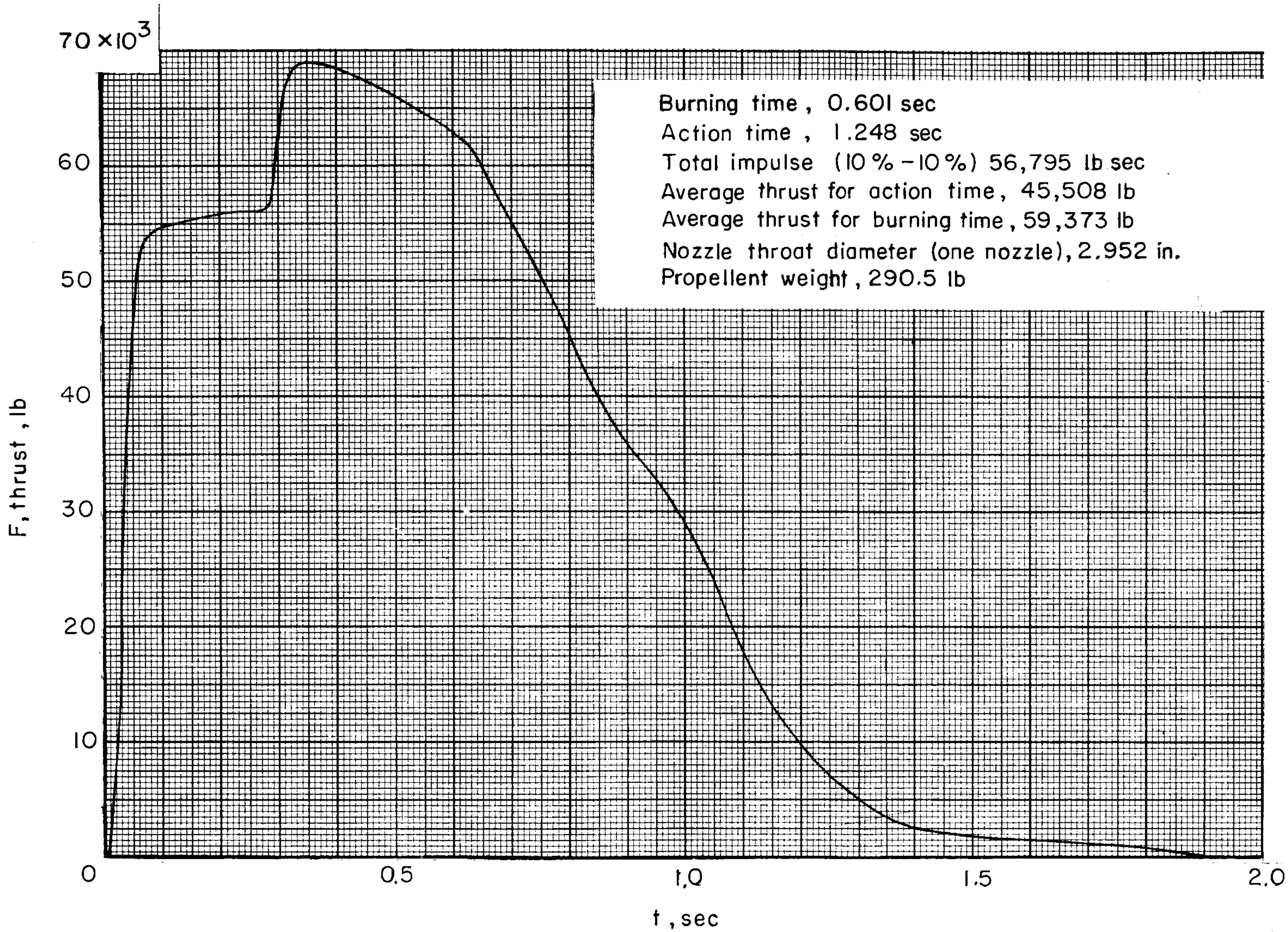

Figure 9.- Typical variation of thrust with time for capsule motor with three nozzles.

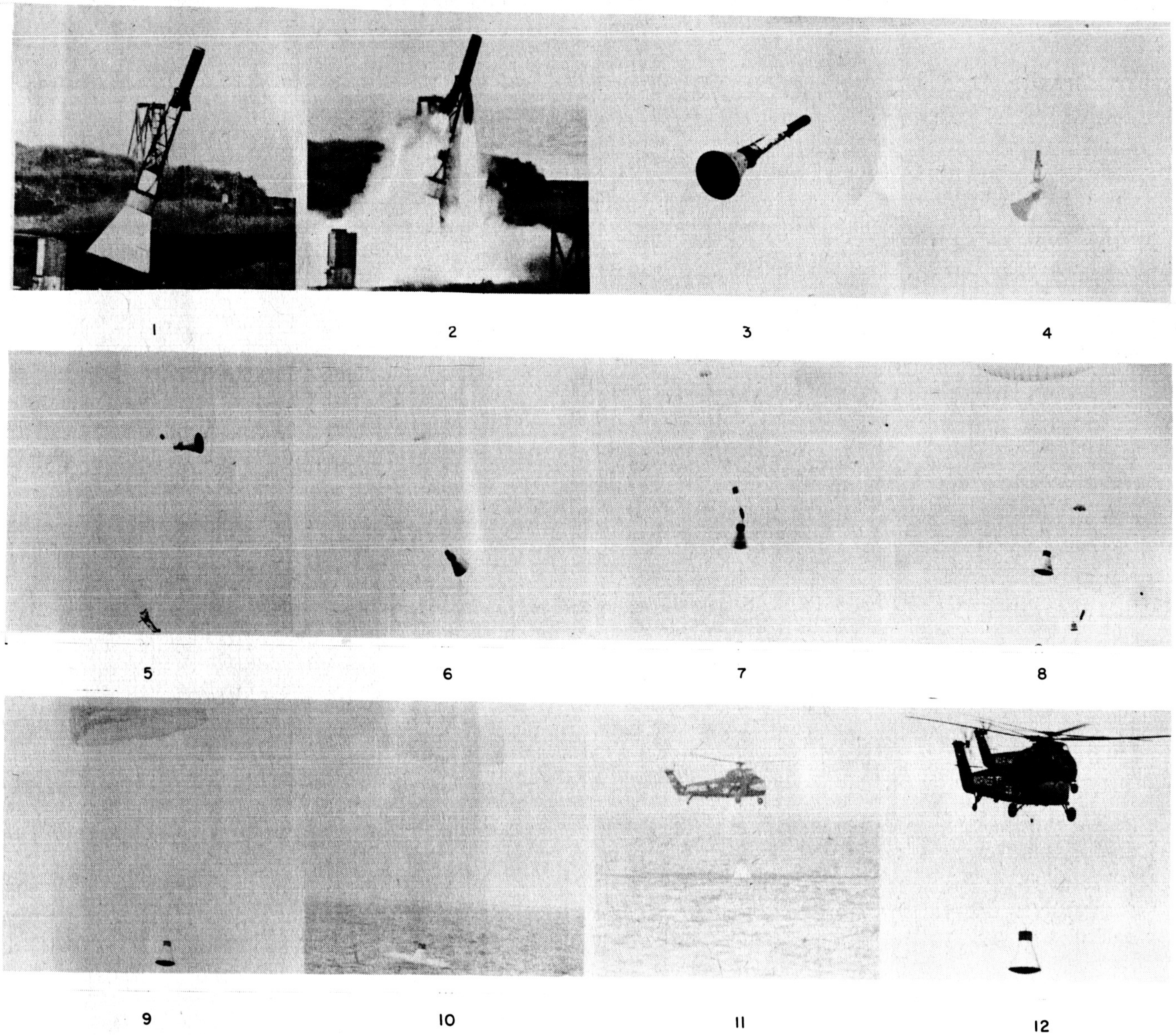

L-60-893
Figure 10.- Sequence photographs of the capsule flight test.

L-1133

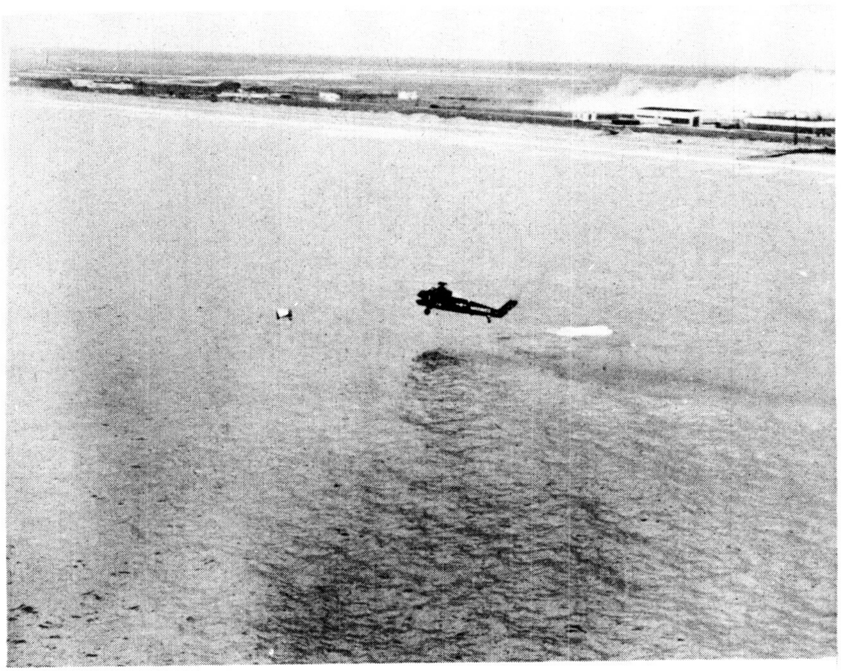

L-59-5452

L-59-5453

Figure 11.- Photographs of helicopter in recovery area.

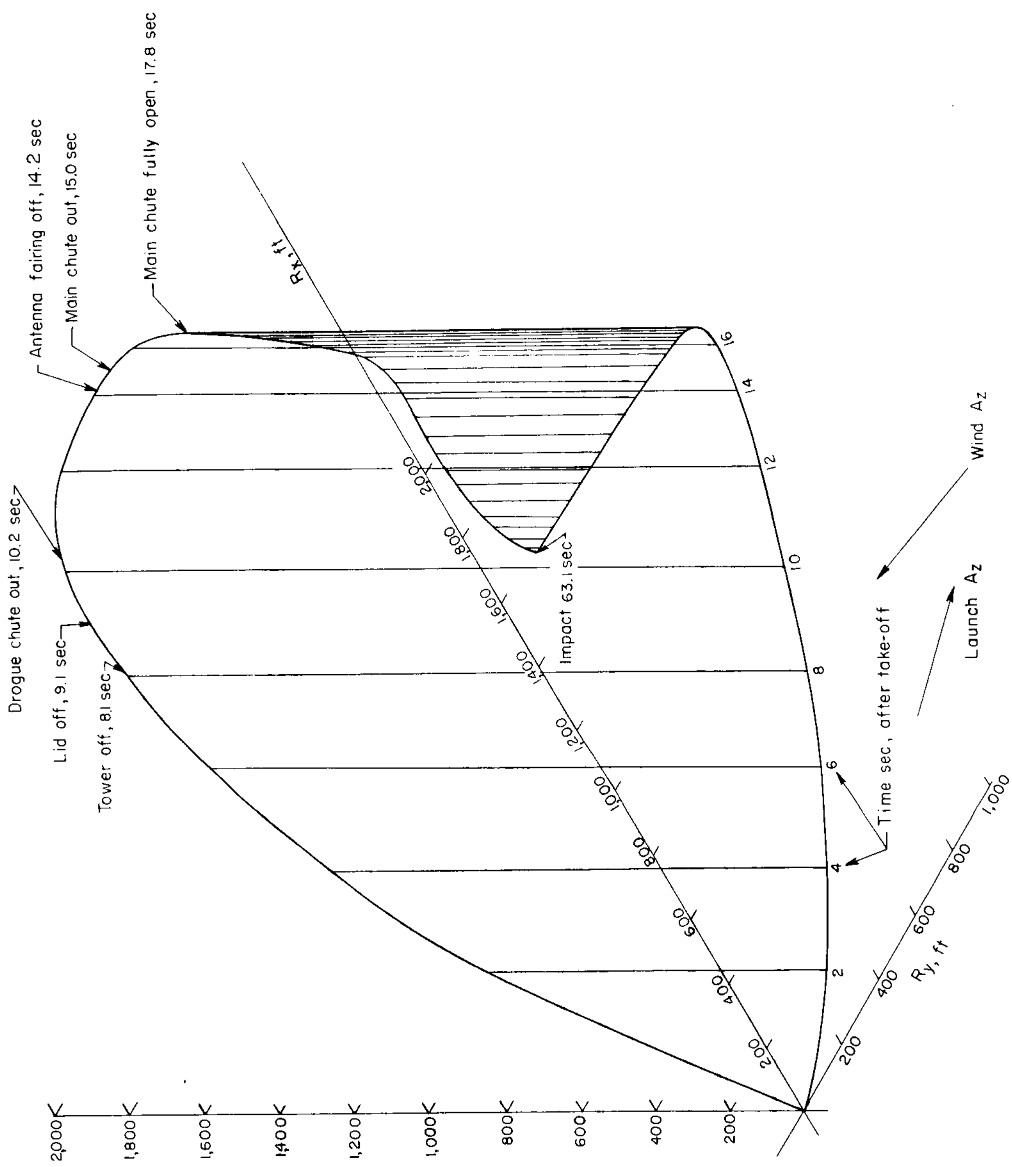

Figure 12.- Isometric trajectory of capsule.

[redacted]

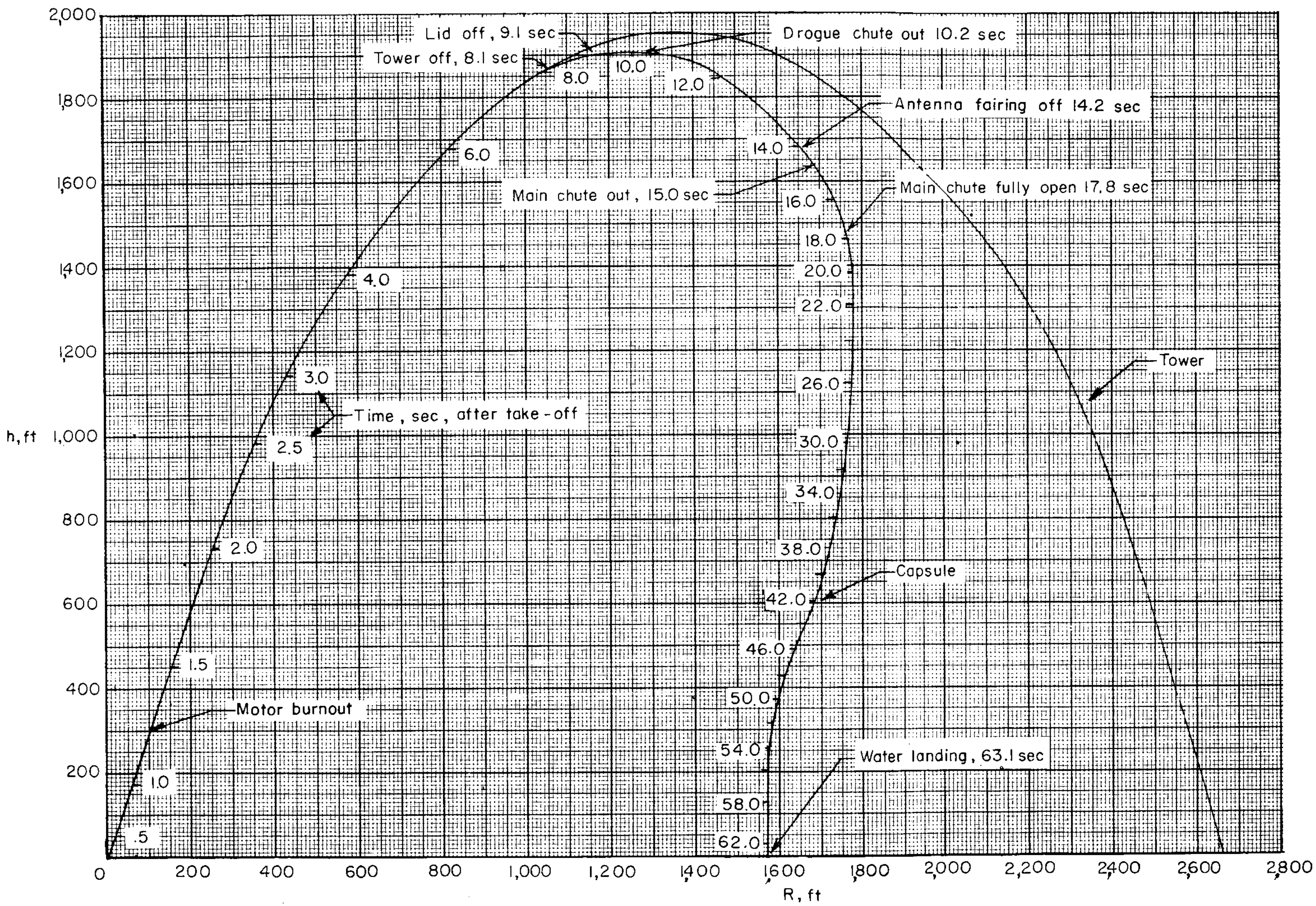

Figure 13.- Variation of altitude with horizontal range.

[redacted]

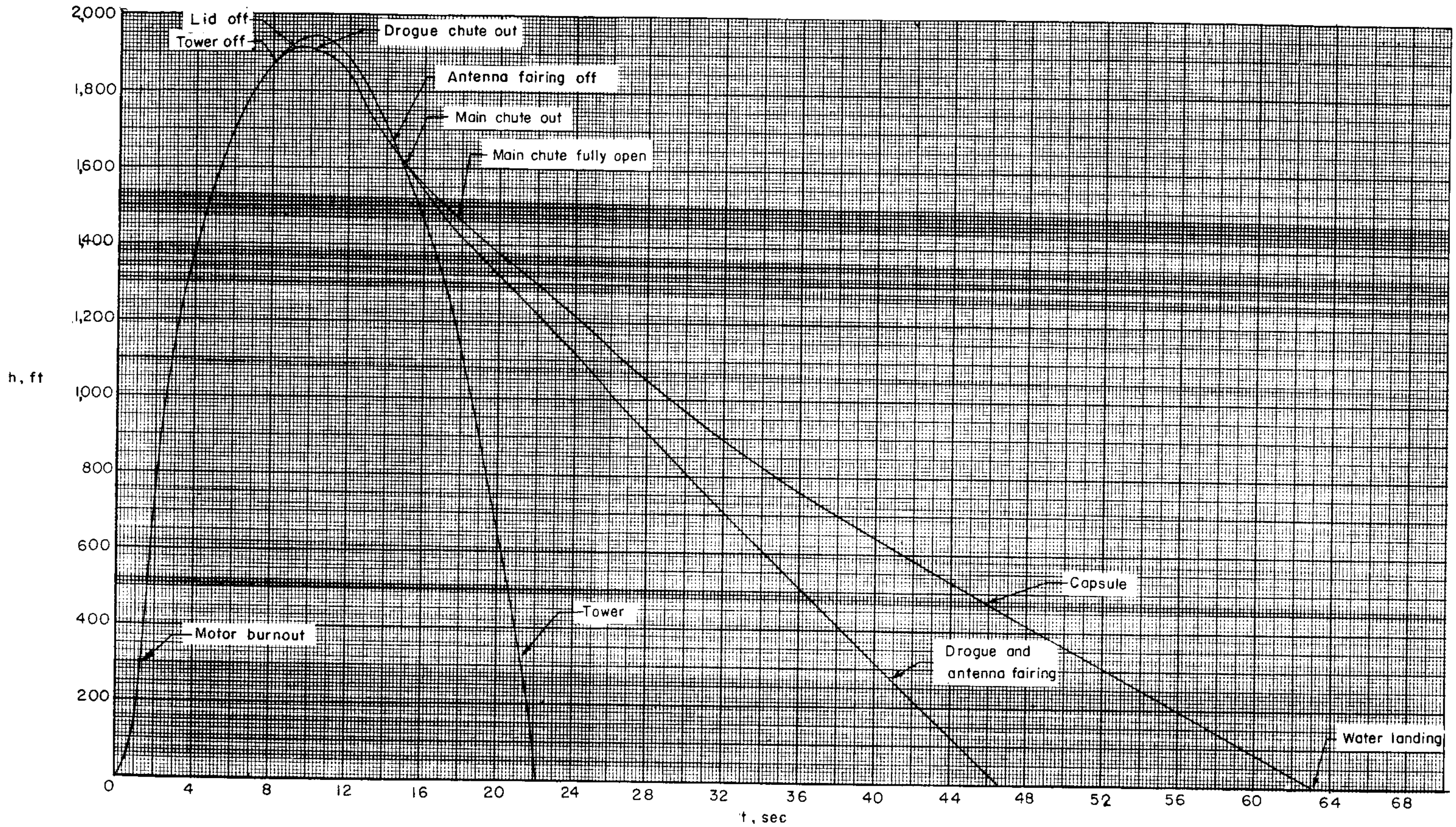

Figure 14.- Variation of altitude with time for capsule, drogue and antenna fairing, and tower.

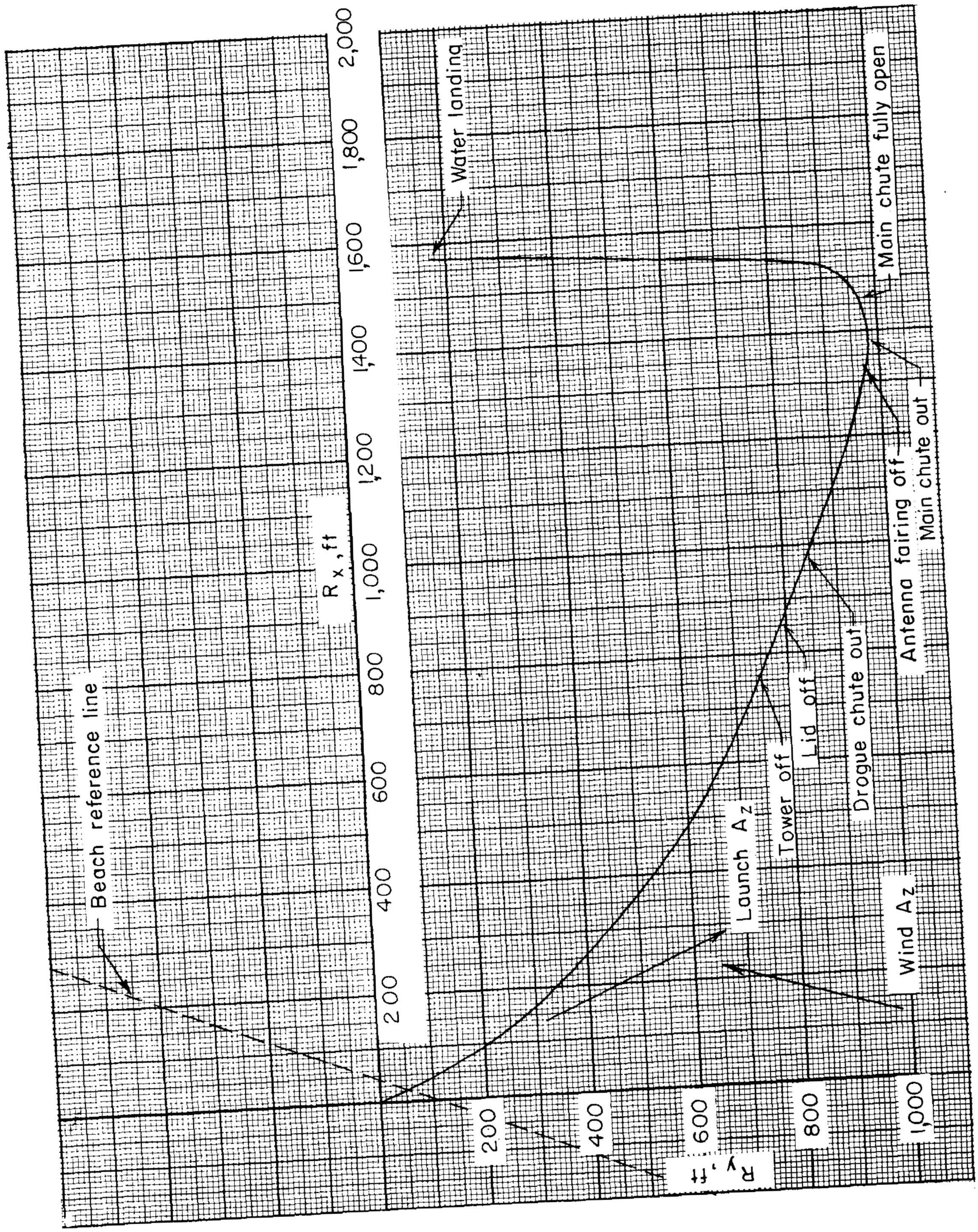

Figure 15.- Ground track of capsule.

[redacted]

[redacted]

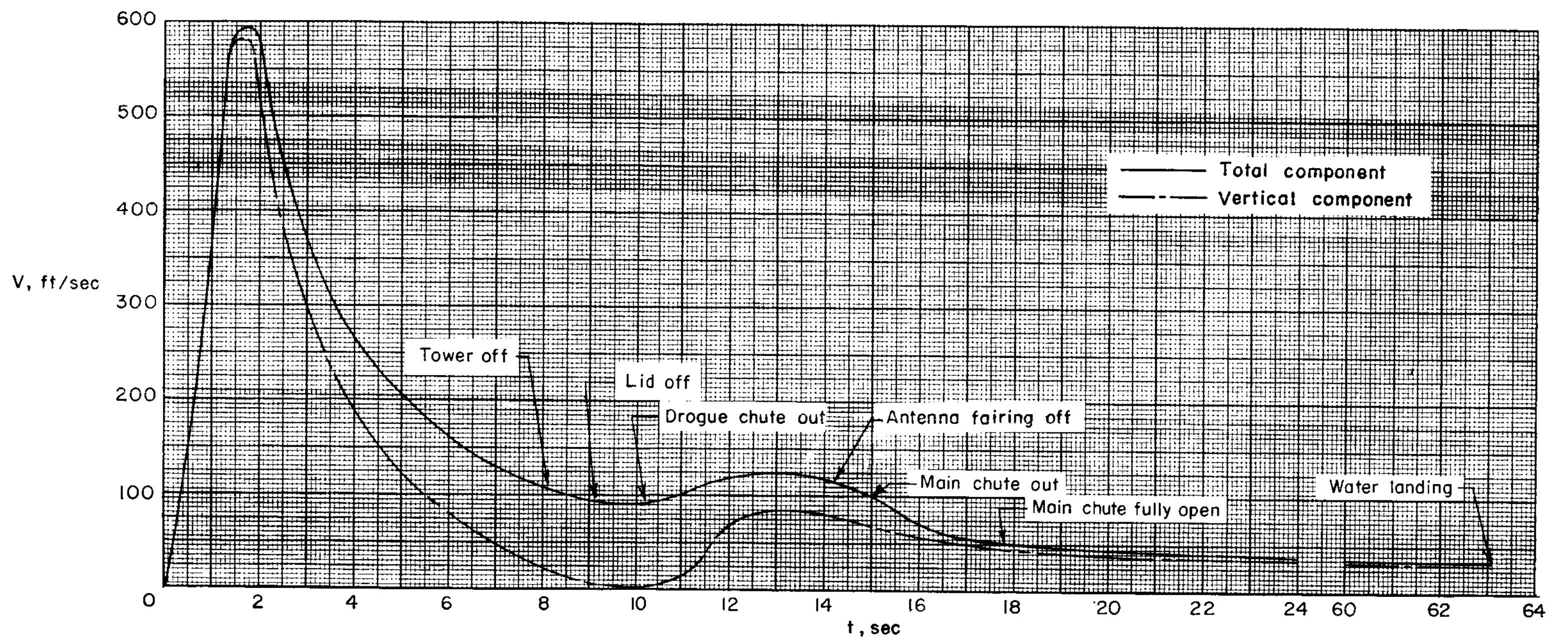

Figure 16.- Variation of velocity with time.

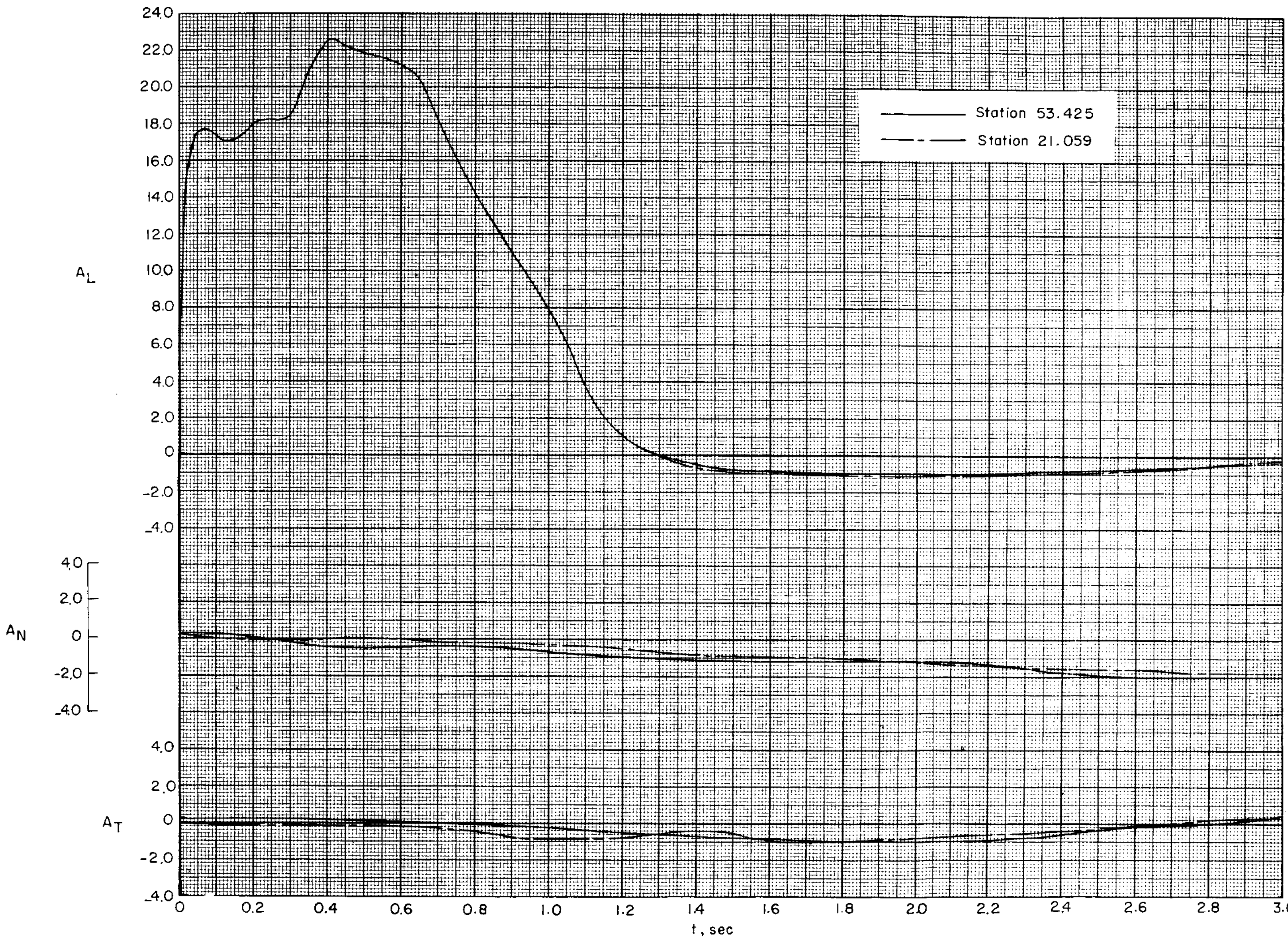

Figure 17.- Variation of longitudinal, normal, and transverse capsule accelerations with time for two axial locations.

[redacted]

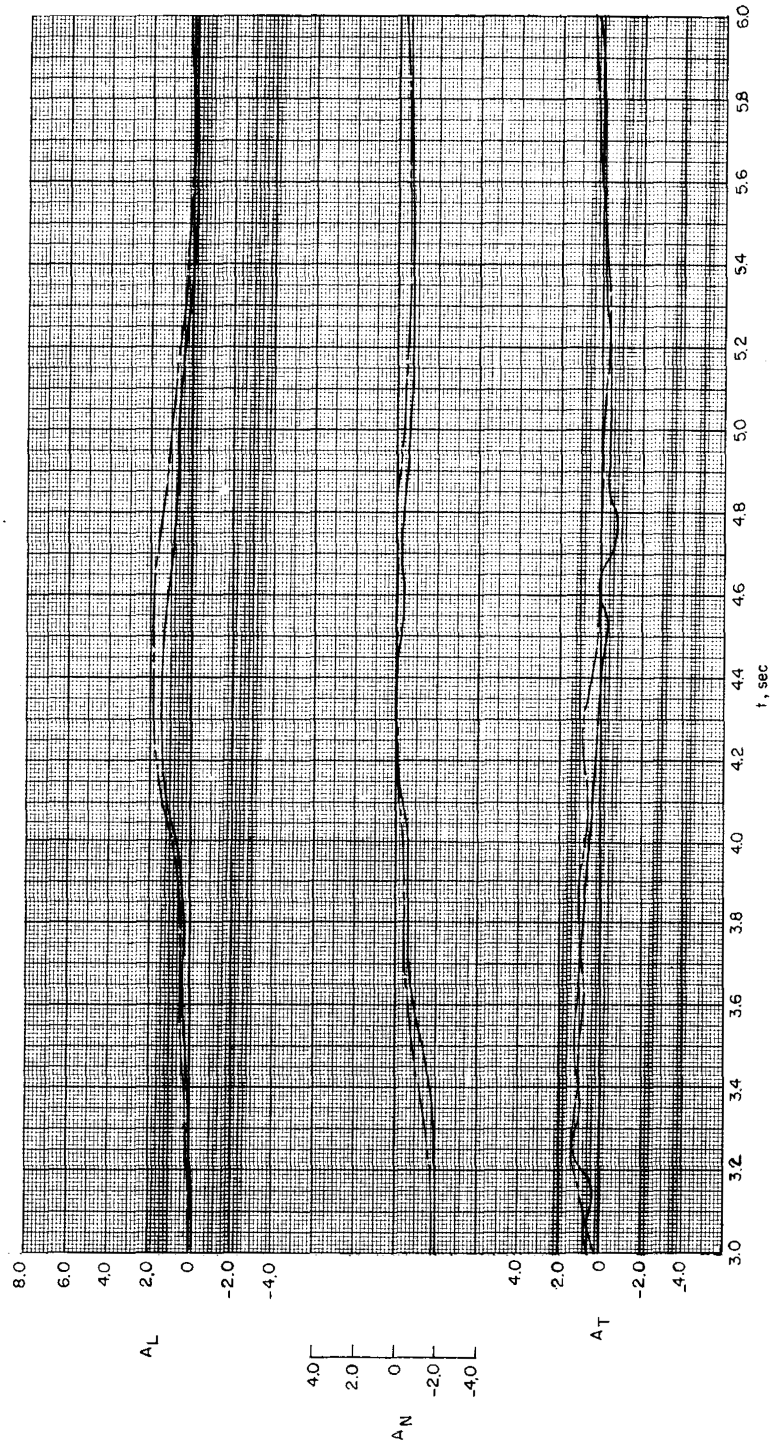

Figure 17.- Continued.

[redacted]

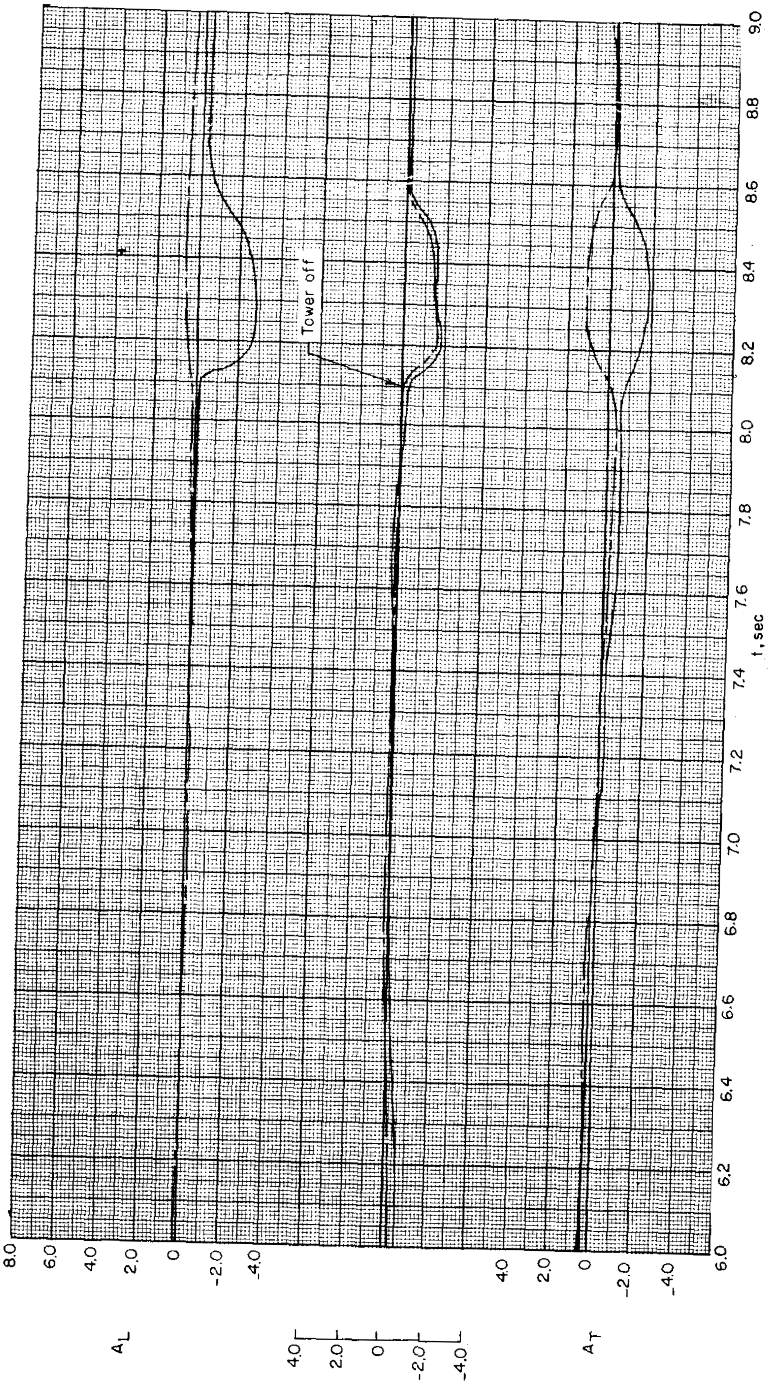

Figure 17.- Continued.

L-1133

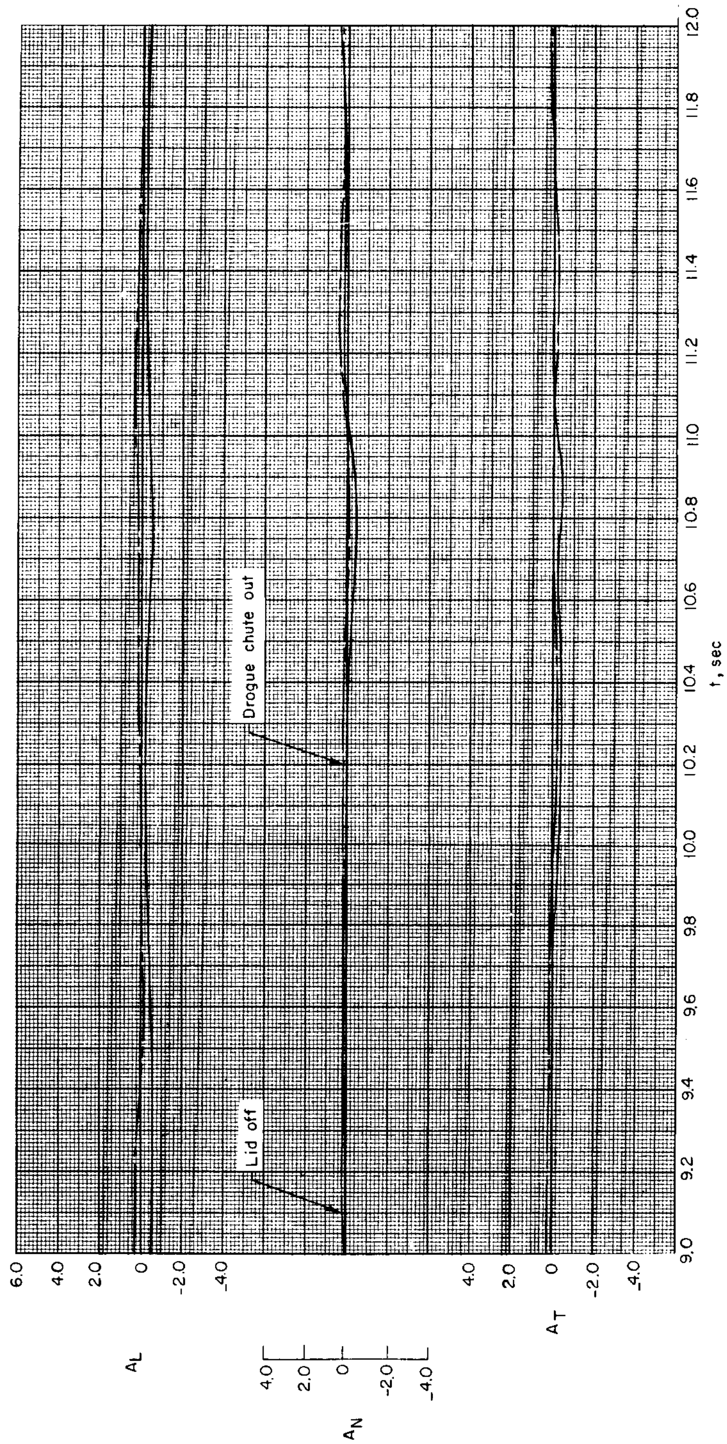

Figure 17.- Continued.

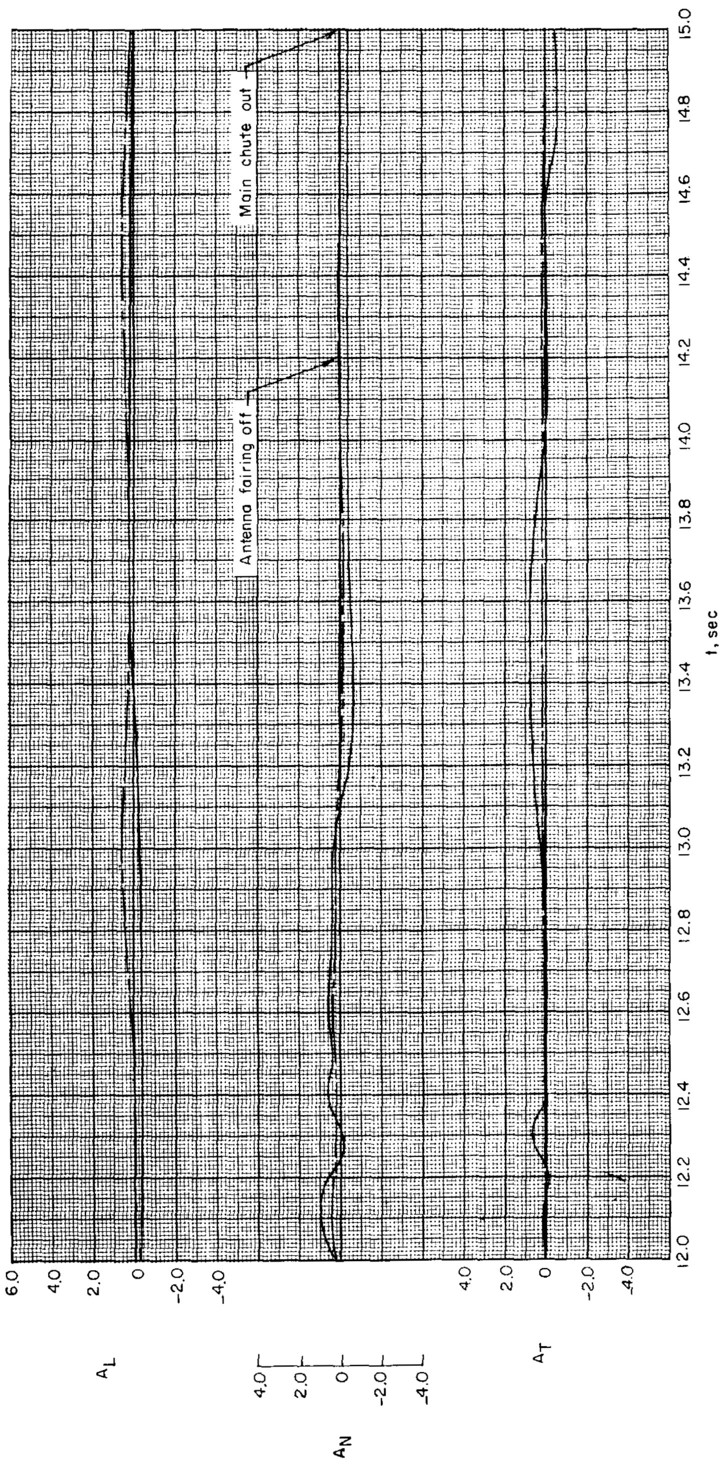

Figure 17.- Continued.

L-1133

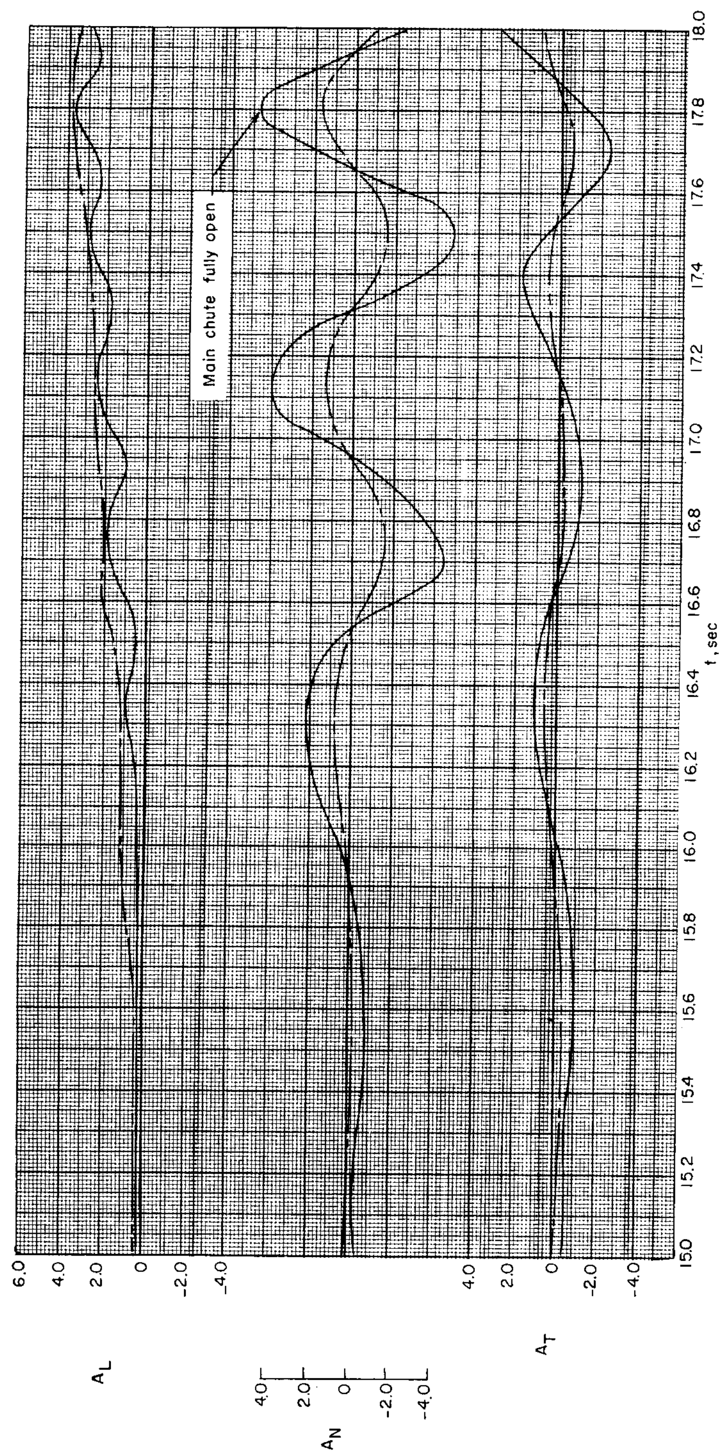

Figure 17.- Continued.

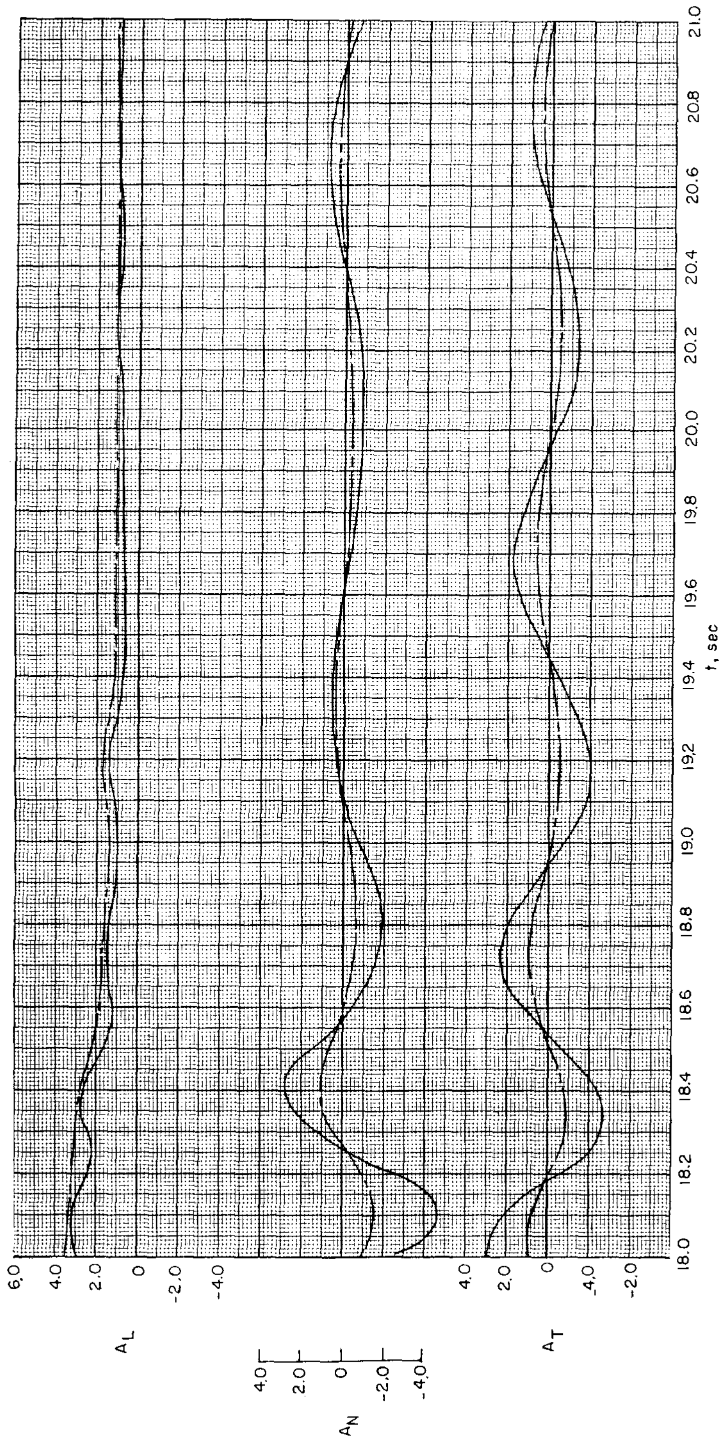

Figure 17.- Continued.

[redacted]

Y

L-1133

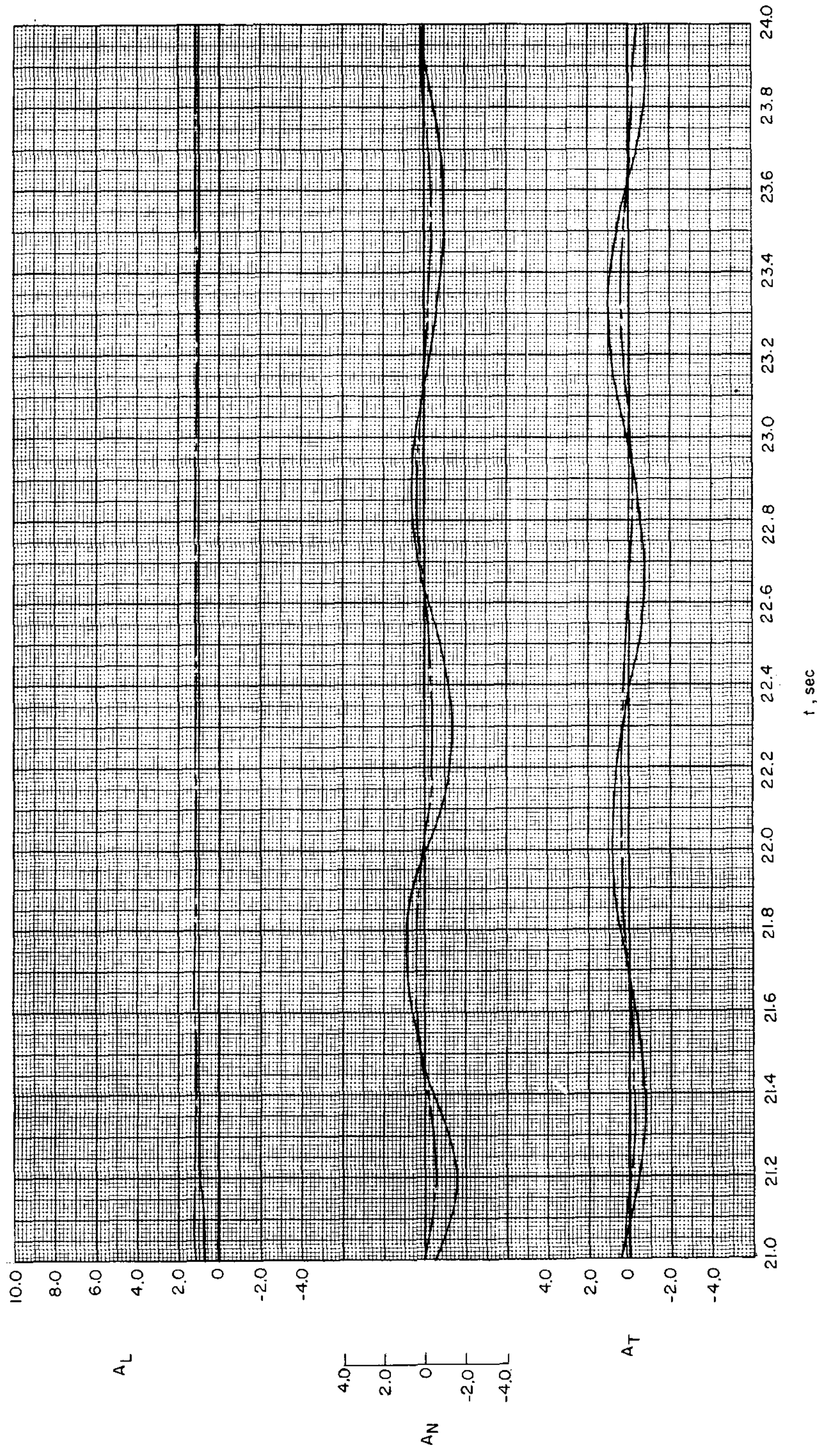

Figure 17.- Concluded.

[redacted]

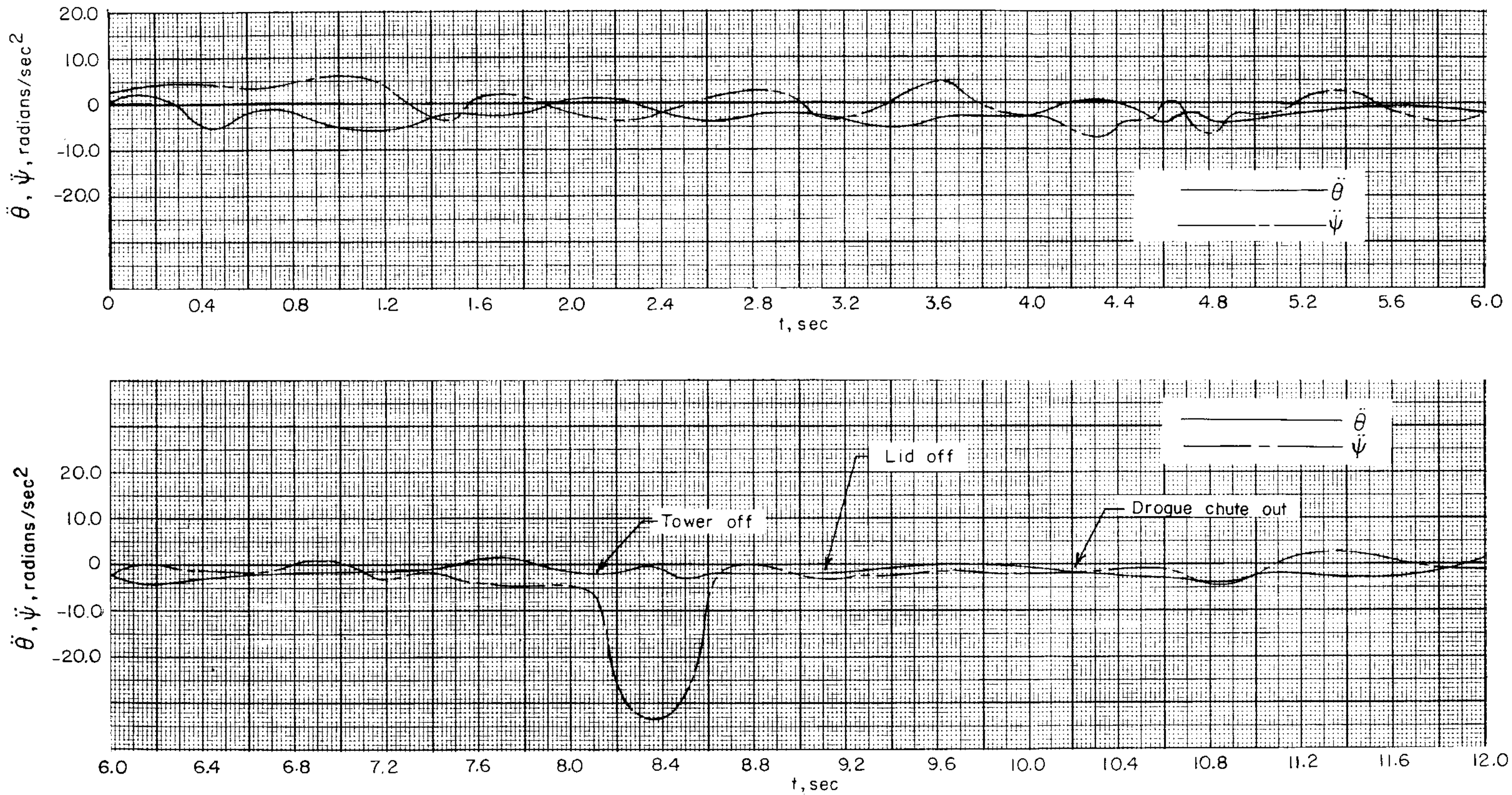

Figure 18.- Variation of pitching and yawing accelerations with time.

[redacted]

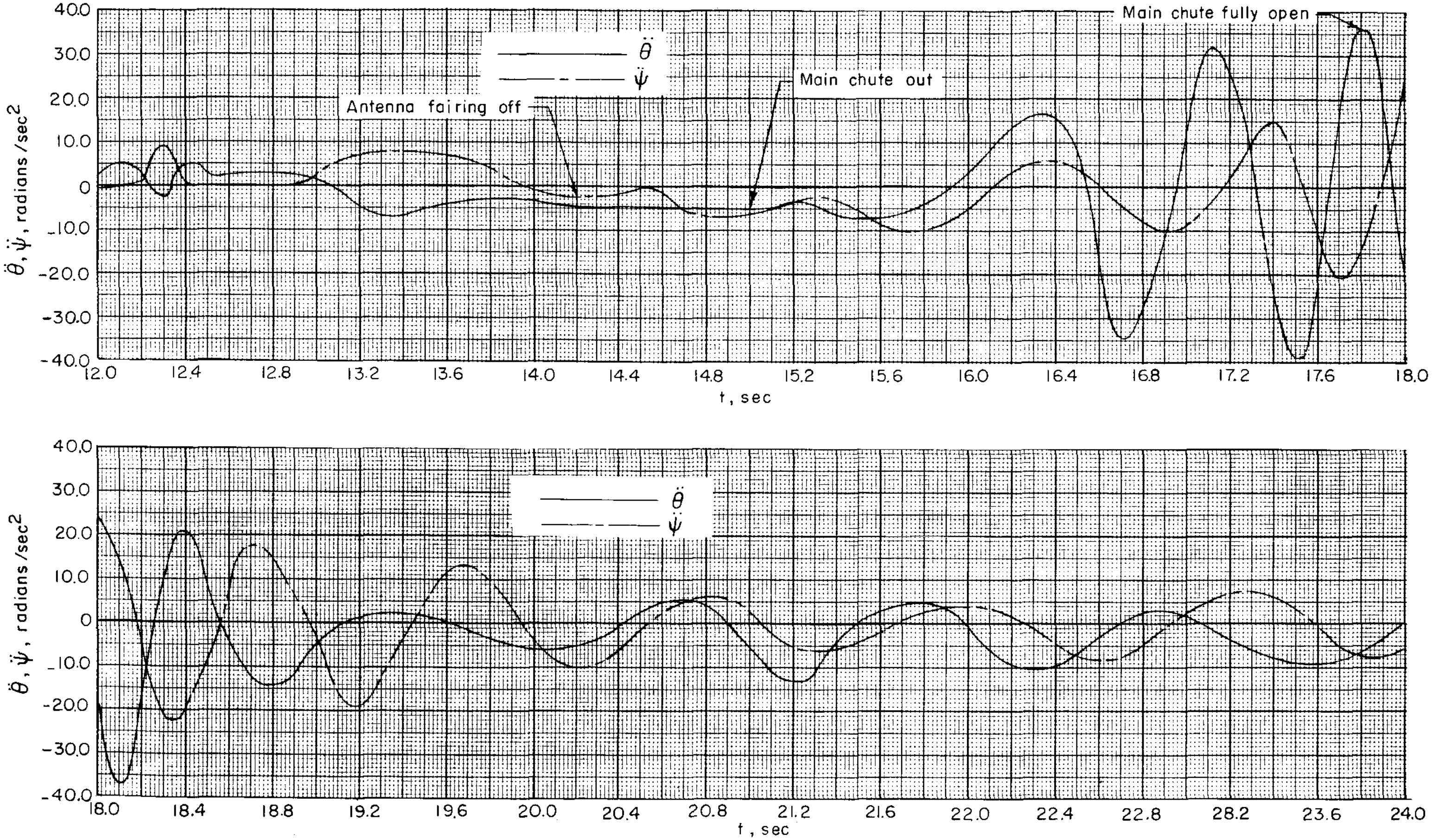

Figure 18.- Continued.

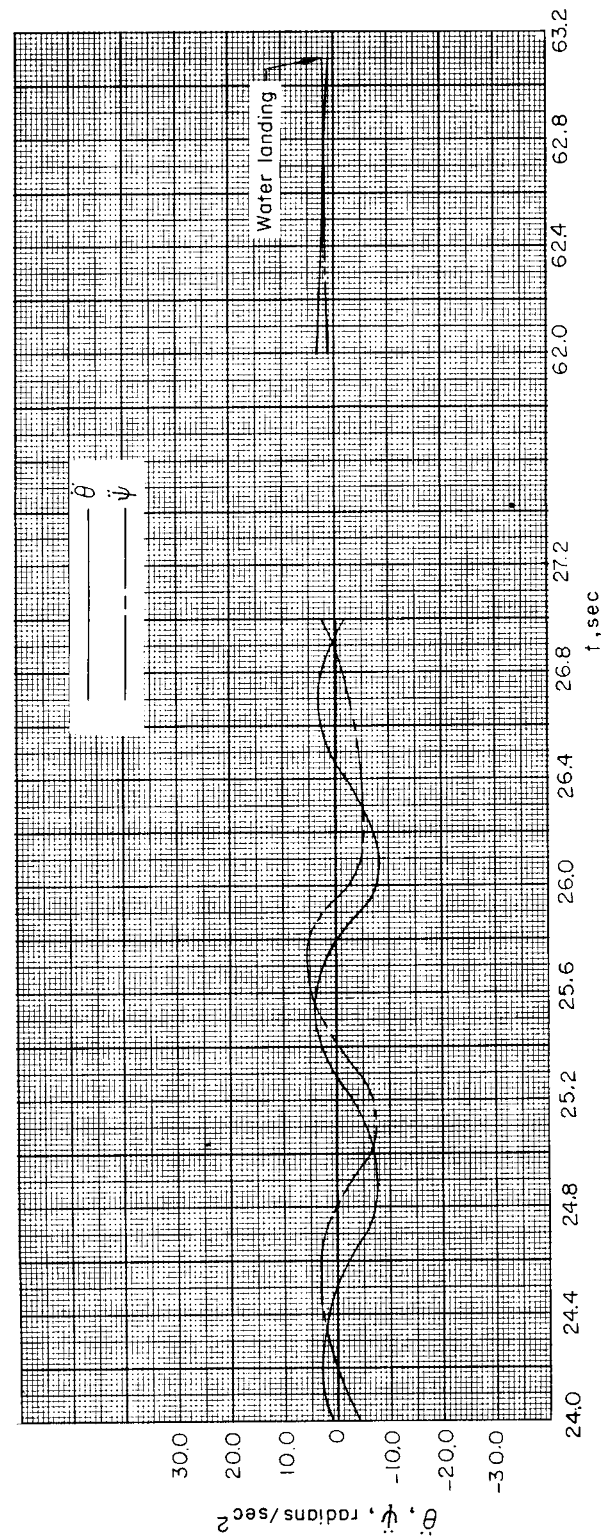

Figure 18.- Concluded.

NASA - Langley Field, Va. L-1133